

Synthesis, Evaluation, and Radiolabeling of New Potent Positive Allosteric Modulators of the Metabotropic Glutamate Receptor 2 as Potential Tracers for Positron Emission Tomography Imaging

José-Ignacio Andrés,^{*,†} Jesús Alcázar,[†] José María Cid,[†] Meri De Angelis,[†] Laura Iturrino,[†] Xavier Langlois,[‡] Hilde Lavreysen,[‡] Andrés A. Trabanco,[†] Sofie Celen,[§] and Guy Bormans[§]

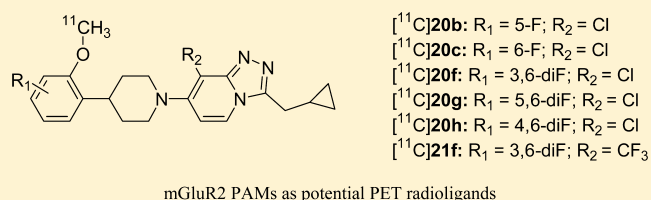
[†]Medicinal Chemistry, Janssen Research & Development, Janssen-Cilag S.A., C/Jarama 75, 45007 Toledo, Spain

[‡]Neuroscience, Janssen Research & Development, Janssen Pharmaceutica N.V., Turnhoutseweg 30, B-2340 Beerse, Belgium

[§]Laboratory for Radiopharmacy and IMIR, Faculty of Pharmaceutical Sciences, K.U. Leuven, Herestraat 49, B-3000 Leuven, Belgium

S Supporting Information

ABSTRACT: The synthesis and in vitro and in vivo evaluation of a new series of 7-(phenylpiperidinyl)-1,2,4-triazolo[4,3-*a*]pyridines, which were conveniently radiolabeled with carbon-11, as potential positron emission tomography (PET) radiotracers for in vivo imaging of the allosteric binding site of the metabotropic glutamate (mGlu) receptor subtype 2 are described. The synthesized compounds proved to be potent and selective positive allosteric modulators (PAMs) of the mGlu receptor 2 (mGluR2) in a [³⁵S]GTPγS binding assay and were able to displace an mGluR2 PAM radioligand, which we had previously developed, with IC₅₀ values in the low nanomolar range. The most promising candidates were radiolabeled and subjected to biodistribution studies and radiometabolite analysis in rats. Preliminary small-animal PET (μPET) studies in rats indicated that [¹¹C]20f binds specifically and reversibly to an mGluR2 allosteric site, strongly suggesting that it is a promising candidate for PET imaging of mGluR2 in the brain.



INTRODUCTION

Glutamate is the major excitatory neurotransmitter in the mammalian central nervous system (CNS) and plays a major role in numerous physiological and behavioral processes via two different receptor classes, the ionotropic (iGlu) and the G-protein coupled metabotropic glutamate (mGlu) receptors.^{1,2} There are eight known mGlu receptor subtypes, of which subtype 2 (mGluR2), which belongs to the group II mGlu receptors, is an attractive potential therapeutic target in neuropharmacology. Preferentially expressed on presynaptic nerve terminals, mGluR2 negatively modulates glutamate and GABA release.³ Thus, it may be hypothesized that schizophrenia-like symptoms arising from increased glutamate transmission in the forebrain could be treated by stimulating mGluR2, thereby reducing synaptic glutamate levels.⁴ Based on this mechanism, normalizing glutamate levels by mixed mGluR2/3 agonists has shown comparable efficacy as conventional antipsychotic drugs for treating schizophrenia.⁵ Indeed, clinical validation was achieved in a phase II study in schizophrenic patients with LY2140023, the orally available prodrug of the mixed mGluR2/3 orthosteric agonist LY404039, which demonstrated improvements in both positive and negative symptoms.⁶ In addition, multiple preclinical studies have reported efficacy of mGluR2 activation in animal models of neurologic disorders such as schizophrenia, anxiety/stress, and depression.^{7–10} Furthermore, activating mGluR2/3 has

been shown to be efficacious to treat anxiety disorders in clinical trials.¹¹

A new avenue for developing selective agents acting at mGlu receptors is to identify compounds that act through allosteric mechanisms, modulating the receptor by binding to a site different from the highly conserved orthosteric glutamate binding site. Positive allosteric modulators (PAMs) offer several advantages over orthosteric agonists: the ligands are not based on an amino acid structure, which is generally detrimental for CNS penetration, they avoid the conserved mGluR orthosteric binding site and offer improved selectivity, they may be less liable to cause receptor desensitization, and they only act in the presence of endogenous glutamate, thereby responding to physiological fluctuations.^{12–14} The number of chemically diverse mGluR2 PAMs reported over the last years in both patent applications and research journals has increased dramatically.¹⁵

Noninvasive imaging of mGluR2 using positron emission tomography (PET) would allow quantification of the distribution, expression, and modulation of this receptor under physiological and pathological conditions. PET imaging of mGluR2 would allow better understanding of the role of this receptor under different neuropsychiatric conditions, and it would facilitate the clinical development of mGluR2 modu-

Received: June 28, 2012

Published: September 20, 2012

lators as potential drug candidates by giving direct insight into the relationship between the level of receptor occupancy and the administered dose of the candidate drug.^{16,17} Several PET radiotracers have been reported for in vivo imaging of group I mGluRs (mGluR1 and mostly mGluR5).^{18–21} Very recently the first PET radioligand for imaging group II mGluRs *in vivo* has been reported ($[^{11}\text{C}]$ CMGDE, **1**).²² However, **1** (Figure 1)

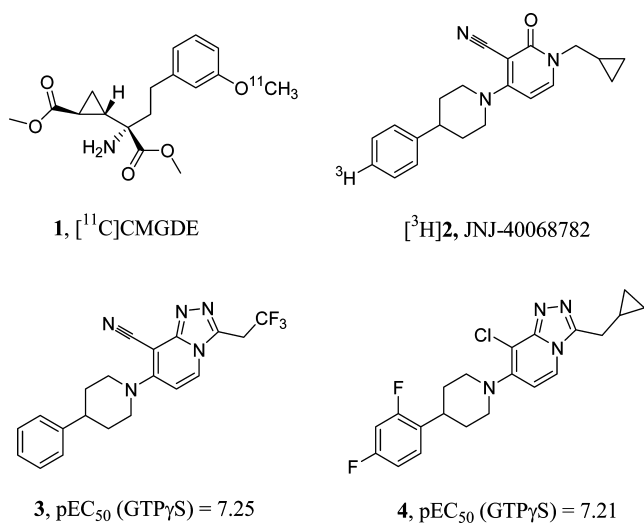


Figure 1. Structures of two mGluR2 radioligands and two 1,2,4-triazolo[4,3-*a*]pyridine mGluR2 PAMs.

shows high affinity for both mGluR2 and mGluR3, and since it binds to the orthosteric binding site, it cannot be used for imaging studies with novel mGluR2 PAM drug candidates. Furthermore, $[^{11}\text{C}]$ CMGDE is in fact a prodrug (dimethylester of an amino acid like molecule) and its brain retention may therefore also reflect esterase activity in the brain; this hypothesis is supported by the fact that blocking studies showed only 20–30% reduced brain uptake. To our knowledge, there is no PET radiotracer disclosed for imaging selectively mGluR2 so far.

We started a research program to develop a PET radiotracer for in vivo imaging of mGluR2 in brain, in parallel to the Medicinal Chemistry efforts aiming at the identification of a suitable mGluR2 PAM for clinical development. We have reported several structurally diverse chemotypes of mGluR2 PAMs.¹⁵ Among them, one of the most exemplified chemical series is the 1,4-disubstituted 2-pyridones.^{15,23} Radiolabeled mGluR2 PAM $[^3\text{H}]$ JNJ-40068782 ($[^3\text{H}]$ **2**, Figure 1) belongs to this chemotype and was recently characterized and described by

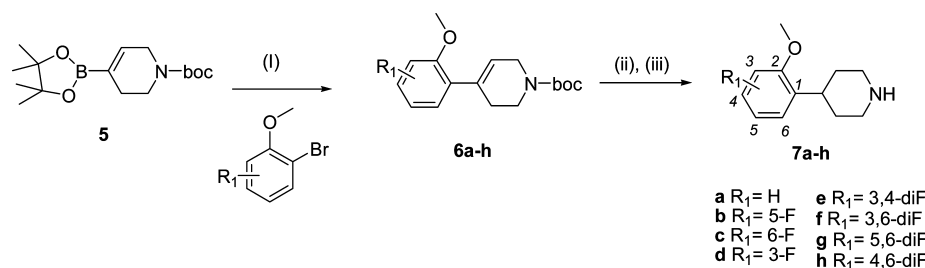
us as a good tool to study allosteric mGluR2 interactions and to explore the relation between receptor binding and function.²⁴ Overall, the PAMs tested showed similar affinity and were able to displace $[^3\text{H}]$ **2** from recombinant human receptors and native rat receptors.²⁴ These promising results prompted us to start a program aiming at the identification of a potential PET radiotracer for in vivo imaging of the mGluR2 allosteric binding site(s). In a first attempt, several analogs of the 4-(phenylpiperidinyl)-2-pyridone derivative **2**, containing different substituents that could be amenable for radiolabeling with either carbon-11 or fluorine-18, were prepared. However, none of the synthesized derivatives could be taken into consideration as a potential PET radiotracer candidate due to suboptimal potency,^{15,23} as well as low brain uptake (unpublished results). In a second attempt, the 1,2,4-triazolo[4,3-*a*]pyridine chemical series, exemplified by compounds **3** and **4** (Figure 1) was developed, providing compounds with increased potency.²⁵ Previous exploration on the 4-(phenylpiperidinyl)-2-pyridones showed that the introduction of a methoxy substituent on the phenyl ring in the *ortho*-position to the piperidine moiety would not only facilitate the production of the carbon-11 analog but could also increase the mGluR2 PAM potency. Furthermore, the presence of one or two fluorine atoms in different positions of the phenyl ring could impact the compound potency, as well as the metabolic stability and brain penetration.²⁶

Based on these observations, a set of differently substituted 7-[4-(2-methoxyphenyl)-1-piperidinyl]-1,2,4-triazolo[4,3-*a*]pyridines as mGluR2 PAMs that could be easily radiolabeled with carbon-11 were synthesized. The synthesis and in vitro activity of this new series of mGluR2 PAMs, as well as the radiosynthesis of the most promising candidates and their preliminary in vivo evaluation in rats, are reported in this article.

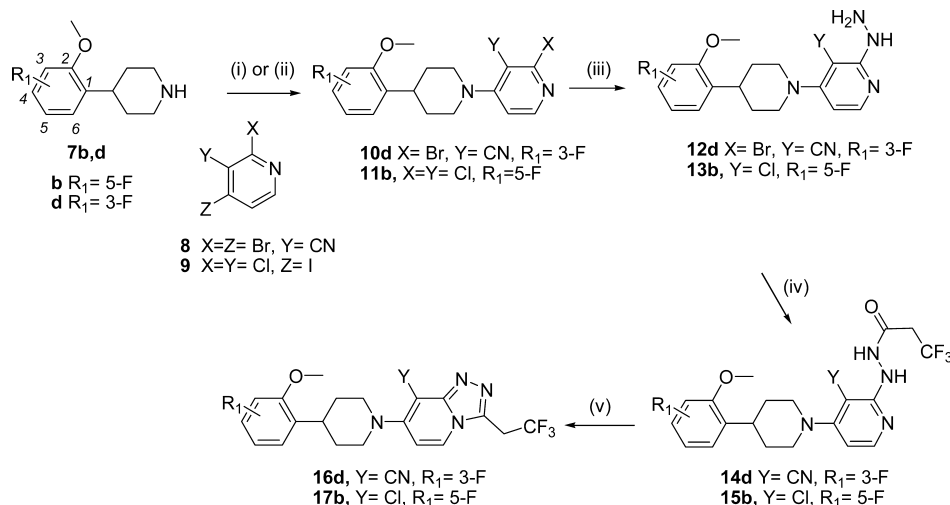
RESULTS AND DISCUSSION

Chemistry and Radiochemistry. Synthesis of key intermediates **7b–h** was achieved in a fast and efficient way using the appropriate synthetic technology depending on the reaction (Scheme 1), following a similar approach as that described in the literature for the synthesis of **7a**.²⁷ In the first step, commercially available boronate **5** was coupled with different 1-bromo-2-methoxyphenyl derivatives in parallel under microwave irradiation²⁸ to give intermediates **6a–h**. These bromo-methoxy-phenyl compounds were either commercially available or were synthesized according to literature precedents (see Experimental Section). Reduction of the double bond in compounds **6a–h** was effectively performed under flow conditions using an H-Cube reactor, and

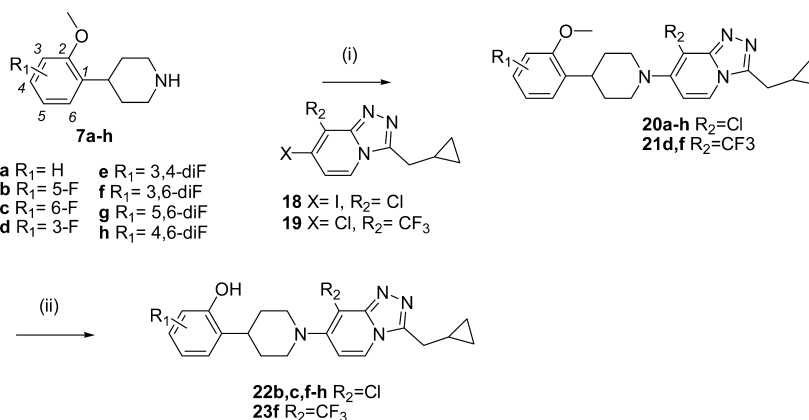
Scheme 1. Synthesis of the Key Intermediates **7a–h**^a



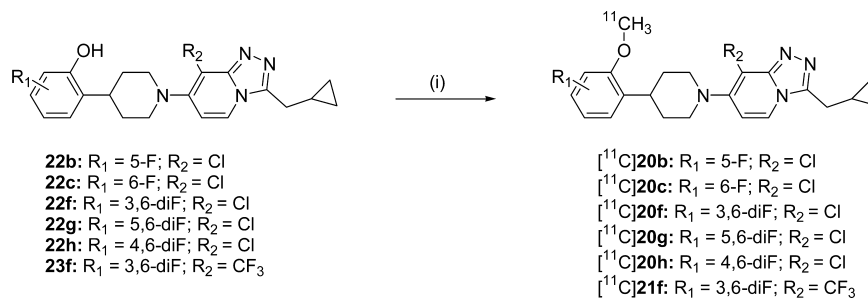
^aReagents and conditions: (i) Pd(PPh₃)₄, K₂CO₃ (saturated solution), 1,4-dioxane, μ W, 150 °C, 10 min; (ii) H₂, EtOH, Pd(OH)₂/C (20%); H-CUBE, full-H₂, 80 °C, 1 mL/min; (iii) HCl (7 M in *i*-PrOH), MeOH, rt, 90 min.

Scheme 2. Synthesis of Final Products 16d and 17b^a

^aReagents and conditions: (i) NaH, DMF, rt, 1 h; (ii) diisopropylamine, MeCN, 110 °C, overnight; (iii) NH₂NH₂, EtOH or THF, μ W, 160 °C, 15–20 min; (iv) CF₃CH₂COCl, Et₃N, CH₂Cl₂, rt, 1 h; (v) POCl₃, MeCN, μ W, 150–160 °C, 5–10 min.

Scheme 3. Synthesis of Final Products 20a–h and 21d,f and Synthesis of the Precursors 22b,c,f–h and 23f^a

^aReagents and conditions: (i) **18** or **19**, Pd(AcO)₂, (±)BINAP, Cs₂CO₃, toluene, 125 °C, overnight; (ii) BBr₃, CH₂Cl₂, rt, 45 min.

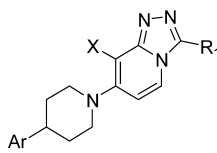
Scheme 4. Radiosynthesis of the Selected PET Tracer Candidates^a

^aReagents and conditions: (i) [¹¹C]CH₃I, Cs₂CO₃, DMF, 90 °C, 3 min, 35–74% RCY.

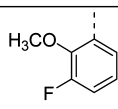
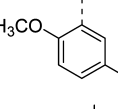
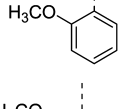
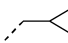
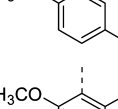
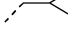
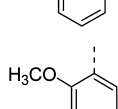

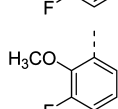

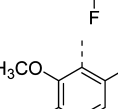

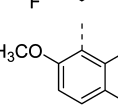

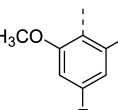

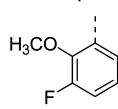

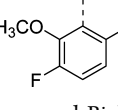
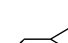
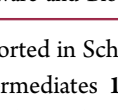
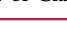
subsequent deprotection of the *tert*-butoxycarbonyl protecting group afforded the desired compounds **7a–h** in good yields. From the above intermediates, two sets of final compounds could be generated. The first set is represented by compounds containing the 3-(2,2,2-trifluoroethyl)-1,2,4-triazolo[4,3-*a*]pyridine fragment and were synthesized from intermediates **7b,d** as starting material (Scheme 2). In a first step, derivatives **7b,d** were *N*-arylated with the substituted pyridines **8**²⁹ or **9** to

give derivatives **10d** and **11b**. Subsequent reaction with hydrazine under microwave conditions afforded intermediates **12d** and **13b**, which were subjected to an acylation reaction with CF₃CH₂COCl to introduce the 2,2,2-trifluoroethyl residue, yielding **14d** and **15b**. Finally, cyclization using microwave irradiation provided the target compounds **16d** and **17b**. The second set of compounds, containing the 3-(cyclopropylmethyl)-1,2,4-triazolo[4,3-*a*]pyridine fragment,

Table 1. Functional Activity of the Synthesized mGluR₂ PAMs



16d, 17b, 20a-h, 21d, 21f

Compd	X	Ar	R ₁	clogP ^a	mGluR ₂ EC ₅₀ (GTPγS) (nM) ^b	mGluR ₂ E _{max} (GTPγS) (%) ^b
16d	CN		CH ₂ CF ₃	2.93	31	306
17b	Cl		CH ₂ CF ₃	4.35	10.5	340
20a	Cl			4.57	20	345
20b	Cl			4.85	8.2	283
20c	Cl			4.85	6.0	304
20d	Cl			4.65	37	336
20e	Cl			4.77	26	342
20f	Cl			4.84	7.5	282
20g	Cl			4.97	9.3	258
20h	Cl			5.04	6.9	256
21d	CF ₃			4.85	11	528
21f	CF ₃			5.04	4.1	421

^aclogP values were calculated from Daylight software and Biobyte, Inc. of Claremont, CA. ^bValues are means of 2–4 experiments.

was synthesized according to the strategy reported in Scheme 3. Intermediates **7a–h** were coupled with intermediates **18**³⁰ or **19**³¹ under Buchwald conditions, providing the target compounds **20a–h** and **21d,f**. Demethylation of selected

compounds was performed in the presence of boron tribromide, to give derivatives **22b,c,f–h** and **23f**, which were used as precursors to prepare the appropriate radiolabeled analogues. In view of the in vitro pharmacological results (see

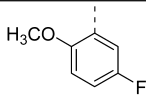
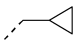
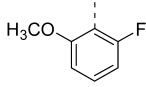
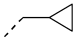
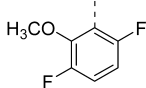
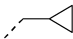
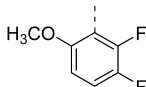
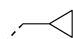
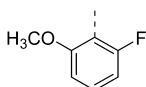

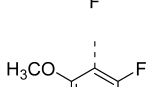

Pharmacology section), derivatives **20b,c,f–h** and **21f** were selected as potential PET radioligands for imaging of mGluR2. Their radiolabeled analogues [^{11}C]**20b,c,f–h** and [^{11}C]**21f** were prepared by methylation of the hydroxyl precursors **22b,c,f–h** and **23f** with [^{11}C]MeI in the presence of cesium carbonate in DMF (Scheme 4). The crude radiolabeling mixtures were purified using reverse phase-HPLC (RP-HPLC), affording [^{11}C]**20b,c,f–h** and [^{11}C]**21f** in 35%–74% radiochemical yields (relative to starting radioactivity of [^{11}C]MeI, nondecay corrected). The radiochemical purity of all six tracers was examined using RP-HPLC and was superior to 96%. The good radiochemical yield and purity of the employed radiochemistry procedure thus could allow easy translation to the production of clinical doses. The identity of the radiotracers was confirmed using analytical HPLC after coinjection with their nonradioactive analogues and comparison of the retention time of the observed peaks in the radiometric and UV channel, respectively.

Pharmacology. We evaluated the effect of all target compounds on [^{35}S]GTP γ S binding to the human mGluR2 receptor induced by an EC₂₀-equivalent concentration of glutamate (see Experimental Section) (Table 1). All new derivatives proved to be among the most potent mGluR2 PAMs reported so far, with EC₅₀'s ranging from 4.1 to 37 nM, and E_{max} values ranging from 256% to 528%. It was not obvious to identify structure–activity (SAR) trends within this series of compounds. In general, comparing the 8-chloro-3-(cyclopropylmethyl)-substituted derivatives, it seemed that the introduction of different fluorine atoms on the methoxy-substituted-phenyl ring increased functional potency, although there were some exceptions (37 nM for **20d** and 26 nM for **20e**, compared to 20 nM for the nonfluorinated derivative **20a**). On the other hand, the presence of a fluorine atom in the other position of the phenyl ring that is adjacent to the piperidinyl moiety seemed to increase potency in the [^{35}S]GTP γ S assay, as was observed for **20h** and **21f**. Lipophilicity did not seem to play a crucial role in activity either, as could be deduced from the comparison of clogP values of the target compounds (see Table 1). Usually, moderate lipophilicity in the clogP range of 2.5–3.5 is considered optimal for adequate brain penetration without an excessive level of nonspecific binding.^{32–34} Hence, at first sight most of the synthesized compounds, with the exception of **16d**, might have been too lipophilic for their consideration as potential PET radiotracer candidates. However, based on previous experience searching for the identification of potential PET radiotracers for imaging PDE10A, we did not discard any compounds at this stage.^{35,38} The 8-cyano- derivative **16d** was one of the first compounds that we synthesized, and we decided to check its ability to cross the blood–brain barrier (BBB). Due to its insolubility, brain and plasma levels were studied after a 10 mg/kg oral dose in rats as a suspension, showing that brain levels were below the quantification limits at the four measured time points, 0.5, 1, 2, and 4 h after administration. Plasma levels were also very low, with the mean maximal concentration being 12.6 ng/mL after 2 h. The disappointing results of **16d** led to deprioritization of this 8-cyano-substituted subseries.

The most potent compounds in the functional assay, **20b**, **20c**, **20f–h**, and **21f**, were also subjected to in vitro binding studies using radioligand [^3H]**2**. These experiments showed that all compounds tested displaced the radioligand with IC₅₀ values in the low nanomolar range and that, in general, there was a nice correlation between the binding and the functional

[^{35}S]GTP γ S data (Table 2). Furthermore, the binding data using the radioligand [^3H]**2** suggested that the 7-(phenyl-

Table 2. In-Vitro Binding of mGluR₂ PAMs Derivatives 20b, 20c, 20f–h, and 21f^a

Compd	X	Ar	R ₁	Binding IC ₅₀ (nM) ^b
20b	Cl			11.2
20c	Cl			11.2
20f	Cl			9.23
20g	Cl			7.3
20h	Cl			5.6
21f	CF ₃			

^aExperimental details of the in vitro binding protocol are described in the Experimental Section. ^bValues are means of two or three experiments.

piperidinyl)-1,2,4-triazolo[4,3-*a*]pyridines and the 4-(phenylpiperidinyl)-2-pyridones may bind to the same or a mutually exclusive allosteric site of the mGluR2. These results were very promising for our goal to identify a suitable PET radiotracer from this chemical series.

We decided to select one of these compounds as a representative example to evaluate their potential to cross the BBB, assuming the hypothesis that the structural similarity between all derivatives would warrant comparable behavior in terms of brain penetration. We chose compound **20b** for a fast study in rats to measure brain and plasma levels after a 0.63 mg/kg intravenous (iv) dose at four different time points. This experiment showed a very quick brain uptake with maximum concentration after ~5 min (316 ng/g) followed by a gradual decline up to 1 h (~50 ng/g). The mean brain/plasma ratio was around 1.1 (Figure 2). These results indicated that the compound showed relatively good brain penetration and some brain retention, and thus, this chemical series deserved to be further explored as potential PET tracers.

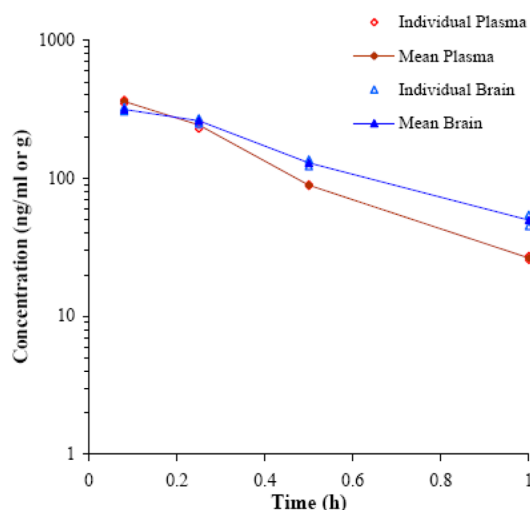


Figure 2. Brain and plasma levels for compound **20b**. Compound was formulated in 20% HP- β -CD. Study was performed in two male Sprague–Dawley rats dosed iv at 0.63 mg/kg. Brain levels are expressed in ng/g and plasma levels in ng/mL. The graphs represent the data as geometric mean values of the two runs.

The mGluR2 selectivity of the final compounds listed in Table 2 was determined using functional receptor assays. Thus, they were tested for agonist and antagonist activity in fluorescent Ca^{2+} assays using HEK293 cells expressing human mGluR1, mGluR3, mGluR5, mGluR7, and mGluR8. Effects on the human mGluR4 and rat mGluR6, expressed in L929 or CHO cells, were assessed in [^{35}S]-GTP γ S functional assays. All compounds displayed mGluR2 selectivity >350–500 fold over the other mGluRs, with the exception of the following compounds, whose selectivity over the mGluR3 receptor was somewhat lower: **20b**, ~40 fold; **20g**, ~70-fold.

We identified the main metabolites formed from the metabolic turnover of some derivatives after incubation with human and rat liver microsomes.³⁷ In both species two major metabolites were observed, one of them being the corresponding O-demethylated derivatives, and the others being M+O oxidative metabolites in which oxidation occurred somewhere on the 3-alkyl-1,2,4-triazolo[4,3-*a*]pyridine fragment. The nonradioactive phenolic derivative formed by O-[^{11}C]-demethylation is thus an expected metabolite for a PET tracer containing a [^{11}C]methoxyphenyl group. As discussed later, the radiometabolite analysis of some of the radiolabeled derivatives showed that only the parent compounds were indeed responsible for brain retention. All the synthesized compounds showed very high plasma protein binding with free fractions lower than 1% in both human and rat plasma, with the exception of **16d** (free fraction 4% and 4.7% in rat and human plasma, respectively). In theory, those levels of plasma protein binding could be considered too high for a suitable PET

radiotracer;³² however, if dissociation from plasma protein occurs fast enough, high plasma protein binding will not be detrimental for adequate brain uptake. Indeed, our previous experience in the PDE10 PET program in which we identified a potential radioligand with plasma protein binding >99.5% prompted us to go ahead with the evaluation of the most promising compounds.³⁵ Also there are different reports in the literature of other successful PET tracers that have a high log *D* and high protein binding but still show good brain penetration.³² Compounds **20b** and **20f** were profiled against ~50 targets in a selectivity screen performed at CEREP.³⁸ Selectivity overall was good, with the only relevant interactions at a 10 μM concentration being dopamine-1 receptor (D1, 71% for **20b** and 76% for **20f**) and the dopamine transporter (DAT, 83% for **20b** and 52% for **20f**). However, both compounds were then tested in-house in a concentration–response curve to measure their affinity, which resulted to be negligible: D1, $K_i \geq 6200$ nM for both compounds; DAT, $K_i = 5005$ nM for **20b** and >8500 nM for **20f**.

Based on all the results shown above, compounds **20b**, **20c**, **20f**, **20g**, **20h**, and **21f**, were selected for radiolabeling with carbon-11.

Biodistribution Studies. All six carbon-11 labeled triazolopyridines ([^{11}C]**20b,c,f-h** and [^{11}C]**21f**) were evaluated in vivo in male healthy Wistar rats by tissue distribution studies at 2, 30, and 60 min postinjection (pi). Table 3 shows the brain uptake of the six tracers at 2 min post-tracer-injection. All tracers produced a similar moderate brain uptake, average 0.71% of the injected dose (ID), with on average 0.52% ID in the cerebrum and 0.16% ID in the cerebellum. Table 4 shows

Table 4. Concentration of [^{11}C]**20f** in Different Rat Brain Regions, Total Brain, and Blood at 2, 30, and 60 min Post-tracer-injection

	SUV ^a		
	2 min	30 min	60 min
striatum	1.22 ± 0.24	2.14 ± 0.38	1.72 ± 0.19
hippocampus	0.90 ± 0.12	1.49 ± 0.33	0.73 ± 0.61
cortex	1.46 ± 0.28	1.77 ± 0.39	1.28 ± 0.24
cerebrum	1.32 ± 0.26	1.96 ± 0.30	1.11 ± 0.60
cerebellum	1.59 ± 0.34	2.62 ± 0.42	1.75 ± 0.36
total brain	1.39 ± 0.24	2.13 ± 0.33	1.18 ± 0.55
blood	0.61 ± 0.09	0.39 ± 0.12	0.28 ± 0.00

^aCalculated as (radioactivity in cpm in organ/weight of organ in grams)/(total cpm recovered/body weight rat in grams). Data are expressed as mean ± SD; *n* = 3 per time point.

the standardized uptake values (SUVs) of the different studied brain regions, the total brain, and the blood for [^{11}C]**20f**. Table 5 presents the relative retention in the studied brain regions for the six tracers. Similar concentrations in brain and blood were

Table 3. Brain Uptake of [^{11}C]**20b,c,f-h** and [^{11}C]**21f** in Normal Rats

	%ID ^a at 2 min pi					
	[^{11}C] 20b	[^{11}C] 20c	[^{11}C] 20f	[^{11}C] 20g	[^{11}C] 20h	[^{11}C] 21f
total brain	0.58 ± 0.03	0.65 ± 0.08	0.88 ± 0.16	0.64 ± 0.13	0.75 ± 0.15	0.75 ± 0.04
cerebrum	0.45 ± 0.03	0.45 ± 0.07	0.69 ± 0.15	0.46 ± 0.11	0.53 ± 0.10	0.54 ± 0.05
cerebellum	0.10 ± 0.00	0.17 ± 0.01	0.17 ± 0.04	0.15 ± 0.05	0.18 ± 0.04	0.17 ± 0.01

^aPercentage of injected dose calculated as counts per minute (cpm) in organ/total cpm recovered. Data are expressed as mean ± SD; *n* = 3 per time point.

Table 5. Wash-out from Different Rat Brain Regions Calculated as 2 min to 30 min Ratio^a for [¹¹C]20b,c,f–h and [¹¹C]21f

	[¹¹ C]20b	[¹¹ C]20c	[¹¹ C]20f	[¹¹ C]20g	[¹¹ C]20h	[¹¹ C]21f
striatum	0.63	0.59	0.57	0.99	0.67	0.86
hippocampus	0.66	0.63	0.60	1.19	0.71	1.01
cortex	0.88	0.71	0.82	0.84	0.66	1.04
cerebrum	0.83	0.60	0.67	0.84	0.72	0.98
cerebellum	0.63	0.71	0.61	0.95	0.77	0.99
total brain	0.79	0.72	0.65	0.93	0.88	1.08

^aCalculated from the 2 and 30 min SUV values.

observed for [¹¹C]20b, [¹¹C]20c, [¹¹C]20g, [¹¹C]20h, and [¹¹C]21f (data not shown). For all studied brain regions, the radioactivity concentration increased from 2 to 30 min pi and the 2-to-30 min wash-out ratios were ≤ 1 for all tracers in all brain regions (except for [¹¹C]20g in the hippocampus 2/30 ratio = 1.19). This accumulation of radioactivity in all studied brain regions is in accordance with the reported intracerebral distribution of mGluR2.³⁹ For all brain regions the radioactivity concentration at 60 min pi was lower compared to the 30 min time point, indicating dissociation of the tracers from their binding site. Since radioactivity was spread throughout the brain, no reference region was available to correct for nonspecific binding in kinetic modeling using a reference tissue model, thus requiring determination of the arterial input function in order to obtain quantitative data. The complete tissue distribution study of [¹¹C]20f is presented in the Supporting Information. At 2 min pi, 4.3% ID was present in blood, and this cleared to 2.0% by 60 min pi. The tracer was cleared mainly by the hepatobiliary system, as there was in total 35.7% of ID present in liver and intestines 60 min after injection of the radiotracer. Because of its extensive plasma protein binding, the urinary excretion of the tracer was minimal with only 2.4% ID present in the urinary system at 60 min pi. A similar clearance pattern was observed for [¹¹C]20b, [¹¹C]20c, [¹¹C]20g, and [¹¹C]20h (data not shown).

Radiometabolite Analysis in Rat Plasma and Perfused Rat Brain. In order to use these PET radioligands for accurate measurements of target density and target occupancy in drug dose occupancy studies, knowledge of radioligand metabolism is required, especially the extent to which radioactive metabolites are present in plasma and their ability to penetrate the brain and contribute to specific and/or nonspecific binding. Therefore, the metabolic stability of [¹¹C]20b, [¹¹C]20f, [¹¹C]20g, and [¹¹C]20h was studied in normal rats by determination of the relative amounts of parent tracer and radiometabolites in plasma and brain at 30 min pi of the tracers.

The reconstructed radiochromatogram of a rat plasma analysis of [¹¹C]20f is included as Supporting Information. From co-injection of the plasma with the authentic reference compound we could identify the peak eluting at ~ 11 min as the intact tracer. The radioactivity corresponding to the more lipophilic fractions eluting after the intact tracer was negligible, indicating the absence of lipophilic radiometabolites, which, if present, could penetrate the BBB. Unidentified polar radiometabolite(s) were eluting from 3 to 6 min. Similar results were found for [¹¹C]20b, [¹¹C]20g, and [¹¹C]20h. An overview of the results of the plasma radiometabolite analysis is presented in Table 6. Of the four ¹¹C-labeled tracers, [¹¹C]20f was found to have the highest fraction ($70 \pm 5\%$) of the recovered

Table 6. Relative Percentages of Intact Tracer and Radiometabolites in Rat Plasma at 30 min Post-injection of [¹¹C]20b, [¹¹C]20f, [¹¹C]20g, and [¹¹C]20h^a

	mean \pm SD			
	[¹¹ C]20b	[¹¹ C]20f	[¹¹ C]20g	[¹¹ C]20h
polar metabolites	59.0 \pm 7.1	30.3 \pm 5.1	54.5 \pm 2.1	69.2 \pm 7.0
intact tracer	41.0 \pm 7.1	69.7 \pm 5.1	45.5 \pm 2.1	30.8 \pm 7.0

^aResults are presented as mean \pm SD; $n = 3$ for [¹¹C]20f, $n = 2$ for [¹¹C]20b, [¹¹C]20g, and [¹¹C]20h.

radioactivity in plasma, present as intact tracer at 30 min post-tracer-injection. The reconstructed radiochromatograms of a perfused rat cerebrum and cerebellum analysis for [¹¹C]20f are also shown in the Supporting Information. The peak corresponding to the intact tracer eluted at ~ 12 min. An overview of the results from the perfused rat brain radiometabolite analysis for [¹¹C]20b, [¹¹C]20f, [¹¹C]20g, and [¹¹C]20h is presented in Table 7. Results were very similar for the four studied tracers. The fraction of apolar radiometabolites detected in brain was negligible. The percentage of polar radiometabolites detected in brain was very small. On average, about 92% of the recovered radioactivity was present as intact tracer in cerebrum and 95% in cerebellum. Future small-animal PET (μ PET) imaging studies will reveal whether this small percentage of radiometabolites in brain needs to be taken into account for determination of quantitative parameters.

Preliminary μ PET Studies. [¹¹C]20f was further evaluated in vivo in normal Wistar rats using μ PET imaging (Figure 3). As was also observed in the biodistribution studies, baseline imaging (Figure 3A,B) showed tracer accumulation in all studied brain regions. The maximum radioactivity concentration (SUV 1.7) in brain was reached at 12 min pi, remained constant until 27 min, and was followed by slow wash-out. After injection of JNJ42153605, a potent PAM discovered by our Janssen R&D team with high affinity and selectivity for mGluR2,⁴⁰ a clear displacement of the radioactivity in all brain regions was observed (Figure 3C,D), demonstrating that the binding of [¹¹C]20f to the mGluR2 allosteric site is reversible and specific.

CONCLUSIONS

In summary, we have synthesized a series of 7-(phenylpiperidinyl)-1,2,4-triazolo[4,3-*a*]pyridines as potent and selective mGluR2 PAMs, which could be radiolabeled with carbon-11 for their evaluation as potential PET radioligands for in vivo imaging of the mGluR2 allosteric binding site. From this investigation we identified several promising candidates that were selected in view of their good potency and selectivity, as well as for their potential to cross the BBB, and they were radiolabeled with [¹¹C]MeI. Biodistribution studies, plasma and brain radiometabolite analysis, and a preliminary μ PET baseline experiment in rats showed that [¹¹C]20f was the most promising PET radioligand candidate for in vivo imaging of mGluR2, due to its good brain uptake and retention and its relatively small fraction of radiometabolites in plasma and brain. The μ PET displacement experiment with a potent and selective PAM discovered by our research team demonstrated that the tracer binding to mGluR2 was specific and reversible. However, due to the widespread distribution of mGluR2 in the brain, no reference region is available for quantification of kinetic parameters and estimation of receptor occupancy. Therefore, extended μ PET imaging studies with [¹¹C]20f are ongoing to

Table 7. Relative Percentages of Intact Tracer and Radiometabolites in Perfused Rat Cerebrum and Cerebellum at 30 min Post-injection of [¹¹C]20b, [¹¹C]20f, [¹¹C]20g, and [¹¹C]20h^a

	[¹¹ C]20b		[¹¹ C]20f		[¹¹ C]20g		[¹¹ C]20h	
	cbr	cbll	cbr	cbll	cbr	cbll	cbr	cbll
polar metabolite	7.6	7.3	9.7 ± 0.3	4.1 ± 1.5	6.9	3.6	7.1	4.5
intact tracer	92.4	92.7	90.3 ± 0.3	95.5 ± 1.3	93.1	96.4	92.9	95.5

^aResults are presented as mean ± SD; *n* = 2 for [¹¹C]20f, *n* = 1 for [¹¹C]20b, [¹¹C]20g, [¹¹C]20h. cbr = cerebrum, cbll = cerebellum.

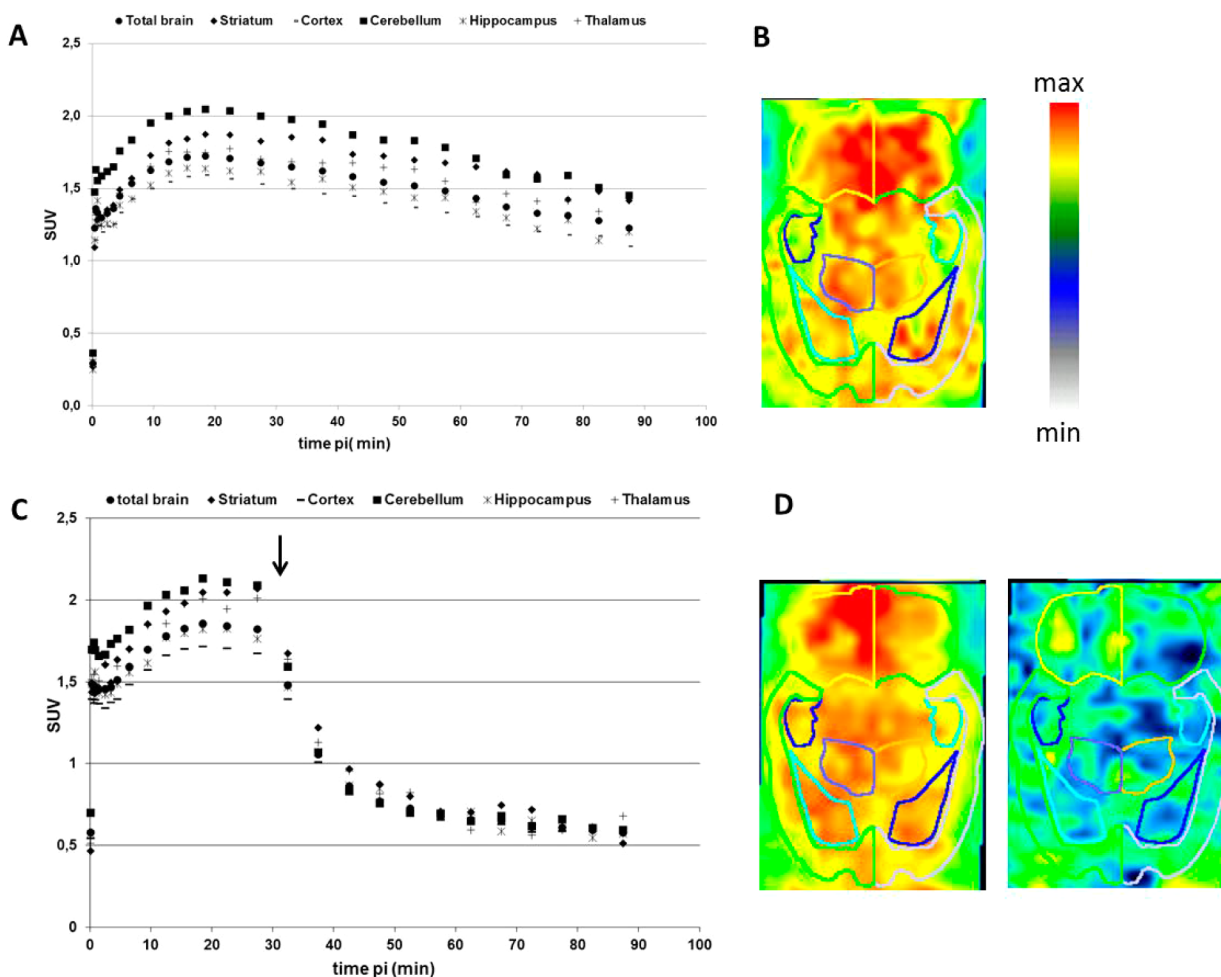


Figure 3. μ PET images and TACs for [¹¹C]20f in rat striatum, cerebellum, cortex, hippocampus, thalamus, and total brain. (A) Untreated baseline scan. (B) Transversal image corresponding to a baseline scan: averaged image (12–28 min after pi) of a representative rat injected with 41 MBq of [¹¹C]20f. (C) Chase experiment: JNJ42153605, 1 mg/kg, was injected iv (arrow) 30 min pi. (D) Transversal images corresponding to the chase experiment: averaged image (12–28 min pi) before chase injection (left) and averaged image (68–88 min pi) after chase injection (right). max = maximum; min = minimum.

further evaluate the kinetics of this tracer and its potential for human brain imaging, the results of which will be reported elsewhere.

EXPERIMENTAL SECTION

Chemistry and Radiochemistry. Materials and General Methods. Unless otherwise noted, all reagents and solvents were obtained from commercial suppliers and used without further purification. Thin layer chromatography (TLC) was carried out on silica gel 60 F254 plates (Merck). Flash column chromatography was performed on silica gel, particle size 60 Å, mesh = 230–400 (Merck) under standard techniques. Microwave assisted reactions were performed in a single-mode reactor, a Biotage Initiator Sixty microwave reactor (Biotage), or in a multimode reactor, a Micro-SYNTH Labstation (Milestone, Inc.). Nuclear magnetic resonance

(NMR) spectra were recorded with either a Bruker DPX-400 or a Bruker AV-500 spectrometer (Bruker AG) with standard pulse sequences, operating at 400 and 500 MHz, respectively, using CDCl₃ and DMSO-*d*₆ as solvents. Chemical shifts (δ) are reported in parts per million (ppm) downfield from tetramethylsilane (δ = 0). Coupling constants are reported in hertz. Splitting patterns are defined by s (singlet), d (doublet), dd (double doublet), t (triplet), q (quartet), quin (quintet), sex (sextet), sep (septet), or m (multiplet). Liquid chromatography combined with mass spectrometry (LC-MS) was performed either on a HP 1100 HPLC system (Agilent Technologies) or Advanced Chromatography Technologies, composed of a quaternary or binary pump with a degasser, an autosampler, a column oven, a diode-array detector (DAD), and a column, as specified in the respective methods. Flow from the column was split to a MS spectrometer. The MS detector was configured either with an electrospray ionization source or an ES-CI dual ionization source

(electrospray combined with atmospheric pressure chemical ionization). Nitrogen was used as the nebulizer gas. Data acquisition was performed with MassLynx-Openlynx software or with Chemsation-Agilent Data Browser software. Detailed information about the different LCMS methods employed can be found in the Supporting Information. Retention time (t_R) is expressed in minutes. Gas chromatography combined with mass spectrometry (GC-MS) was performed using a 6890 Series gas chromatograph (Agilent Technologies) system comprising a 7683 Series injector and autosampler, a column oven, and a J&W HP-5MS, coupled to a 5973N MSD mass selective detector (single quadrupole, Agilent Technologies). The MS detector was configured with an electronic impact ionization source/chemical ionization source (EI/CI). EI low-resolution mass spectra were acquired by scanning from 50 to 550 at a rate of 14.29 scans/s. The source temperature was maintained at 230 °C. Helium was used as the nebulizer gas. Data acquisition was performed with Chemstation-Open Action software. Melting point (mp) values are peak values, were obtained with experimental uncertainties that are commonly associated with this analytical method, and were determined in open capillary tubes on a Mettler FP62 apparatus with a temperature gradient of 10 °C/min. The maximum temperature was 300 °C. The melting point was read from a digital display.

The purities of all new compounds were determined by analytical reverse phase RP-HPLC using the area percentage method on the UV trace recorded at a wavelength of 254 nm, and compounds were found to have $\geq 95\%$ purity unless otherwise specified. For carbon-11 labeled compounds, HPLC analysis was performed on a LaChrom Elite HPLC system (Hitachi, Darmstadt, Germany). The HPLC eluate after passage through the UV detector was led over a shielded 3-in. NaI(Tl) scintillation detector connected to a multichannel analyzer (Gabi box, Raytest, Straubenhardt Germany). The output signal was recorded and analyzed using a GINA Star data acquisition system (Raytest, Straubenhardt, Germany).

4-(3,6-Difluoro-2-methoxyphenyl)-3,6-dihydro-2H-pyridine-1-carboxylic Acid tert-Butyl Ester (6f). Step 1: to a solution of 2,5-difluorophenol (2.0 g, 15.37 mmol) and isopropylamine (1.61 mL, 15.37 mmol) in dry THF (40 mL) was added NBS (3.01 g, 16.19 mmol) portionwise at -40 °C. The reaction mixture was stirred at that temperature for 30 min and then allowed to reach rt. The resulting mixture was diluted with HCl (1 N in H₂O) and Et₂O, the organic layer was separated and dried (Na₂SO₄), and the solvent was evaporated *in vacuo* to yield intermediate 2-bromo-3,6-difluorophenol (3.23 g, 51% pure) that was used as such in the next reaction step. ¹H NMR (500 MHz, CDCl₃) δ 5.71 (br s, 1 H), 6.69 (ddd, $J = 9.2, 7.7, 4.2$ Hz, 1 H), 7.05 (td, $J = 9.5, 4.9$ Hz, 1 H).

Step 2: to a solution of 2-bromo-3,6-difluorophenol (3.23 g, 15.45 mmol) in dry MeCN (25 mL) were added K₂CO₃ (6.4 g, 46.36 mmol) and MeI (2.88 mL, 46.36 mmol), and the resulting mixture was heated under microwave irradiation at 150 °C for 10 min. Then the mixture was diluted with DCM and filtered off, and the filtrate was evaporated *in vacuo* to yield crude 2-bromo-1,4-difluoro-3-methoxybenzene that was used without further purification in the next reaction step. C₇H₃BrF₂O₃. GCMS: Rt 6.67, m/z 223 [M]⁺ (major product).

Step 3: 2-bromo-1,4-difluoro-3-methoxybenzene obtained from the previous step (crude material) was added to a stirred mixture of 3,6-dihydro-4-(4,4,5,5-tetramethyl-1,3,2-dioxaborolan-2-yl)-1(2H)-pyridinecarboxylic acid, 1,1-dimethylethyl ester (**5**, 1.26 g, 4.08 mmol), Pd(PPh₃)₄ (0.07 g, 0.06 mmol), and a saturated aqueous solution of K₂CO₃ (3.5 mL) in 1,4-dioxane (7 mL). The reaction mixture was heated under microwave irradiation at 150 °C for 10 min. After cooling, the mixture was diluted with water and extracted with Et₂O. The organic phase was separated and dried (Na₂SO₄), and the solvent was evaporated *in vacuo*. The crude product was purified by column chromatography (silica gel; EtOAc in heptane 10/90 to 20/80). The desired fractions were collected and concentrated *in vacuo* to give a residue that was triturated with Et₂O to yield compound **6f** as a sticky oil (0.23 g, 22%). C₁₇H₂₁F₂NO₃. LCMS: Rt 3.25, m/z 326 [(M + H)]⁺. ¹H NMR (400 MHz, CDCl₃) δ 1.50 (s, 9 H), 2.38 (br s, 2 H), 3.63 (br s, 2 H), 3.87 (d, $J = 1.6$ Hz, 3 H), 4.06 (br s, 2 H), 5.72 (br s,

1 H), 6.74 (td, $J = 8.9, 3.9$ Hz, 1 H), 6.95 (ddd, $J = 10.6, 9.2, 5.1$ Hz, 1 H).

In a similar manner, compounds **6b-e,g,h** were also synthesized, whereas **6a** is described in the literature.²⁵

tert-Butyl 4-(5-Fluoro-2-methoxyphenyl)-3,6-dihydropyridine-1(2H)-carboxylate (6b). Starting from 2-bromo-4-fluoroanisole (2.28 g, 11.12 mmol) and **5** (2.86 g, 9.26 mmol), compound **6b** (3.4 g, quant yield) was obtained as colorless oil. C₁₇H₂₂FNO₃. LCMS: Rt 3.25, m/z 308 [(M + H)]⁺.

tert-Butyl 4-(2-Fluoro-6-methoxyphenyl)-3,6-dihydropyridine-1(2H)-carboxylate (6c). Starting from 2-bromo-3-fluoroanisole (2.2 g, 10.73 mmol) and **5** (3.01 g, 9.75 mmol), compound **6c** (2.02 g, 67%) was obtained as a colorless oil that solidified on standing. C₁₇H₂₂FNO₃. LCMS: Rt 3.25, m/z 208 [(M - Boc) + H]⁺.

tert-Butyl 4-(3-Fluoro-2-methoxyphenyl)-3,6-dihydropyridine-1(2H)-carboxylate (6d). Starting from 2-bromo-6-fluoroanisole (0.974 mL, 7.31 mmol) and **5** (2.37 g, 7.68 mmol), compound **6d** (1.13 g, 50%) was obtained as a colorless oil. C₁₇H₂₂FNO₃. LCMS: Rt 3.60, m/z 308 [(M + H)]⁺. ¹H NMR (400 MHz, CDCl₃) δ 1.49 (s, 9 H), 2.47 (br s, 2 H), 3.62 (br t, $J = 5.7$ Hz, 2 H), 3.89 (s, 3 H), 4.06 (br d, $J = 2.5$ Hz, 2 H), 5.96 (br s, 1 H), 6.92 (dd, $J = 9.0, 8.6$ Hz, 1 H), 7.04–7.16 (m, 2 H).

tert-Butyl 4-(3,4-Difluoro-2-methoxyphenyl)-3,6-dihydropyridine-1(2H)-carboxylate (6e). Step 1: to a solution of 2,3-difluorophenol (0.50 g, 3.84 mmol) and isopropylamine (0.40 mL, 3.84 mmol) in dry DCM (20 mL) was added NBS (3.01 g, 16.19 mmol) portionwise at -10 °C. The mixture was stirred at that temperature for 30 min and then allowed to reach rt. The reaction mixture was then diluted with HCl (1 N in H₂O), the organic layer was separated and dried (Na₂SO₄), and the solvent evaporated *in vacuo*. The crude compound was purified by chromatography (silica gel, EtOAc in heptane 0:100 to 20:80). The desired fractions were collected and the solvent evaporated *in vacuo* to yield 6-bromo-2,3-difluorophenol (0.63 g, 78%). C₆H₃BrF₂O. GCMS: Rt 6.86, m/z 209 [M]⁺. ¹H NMR (400 MHz, CDCl₃) δ 6.36 (td, $J = 9.4, 7.6$ Hz, 1 H), 6.50 (br s, 1 H), 7.12 (ddd, $J = 8.8, 6.1, 2.4$ Hz, 1 H).

Step 2: 6-bromo-2,3-difluorophenol (0.63 g, 2.99 mmol), MeI (0.281 mL, 4.51 mmol), and K₂CO₃ (0.623 g, 4.51 mmol) in MeCN (87.5 mL) were heated at 150 °C for 10 min in a microwave oven. Then DCM was added, the solid was filtered off, and the filtrate solvent was evaporated under vacuum, affording 1-bromo-3,4-difluoro-2-methoxybenzene (0.62 g, 92%) as a sticky oil that was used as such in the next reaction step. C₇H₃BrF₂O. GCMS: Rt 6.54, m/z 222 [M]⁺. ¹H NMR (500 MHz, CDCl₃) δ 4.00 (d, $J = 1.44$ Hz, 3 H), 6.83 (td, $J = 9.25, 7.51$ Hz, 1 H), 7.23–7.29 (m, 1 H).

Step 3: starting from 1-bromo-3,4-difluoro-2-methoxybenzene (0.86 g, 3.83 mmol) and **5** (0.22 g, 0.19 mmol), compound **6e** was obtained (0.79 g, 63%) as a colorless oil. C₁₇H₂₁F₂NO₃. LCMS: Rt 3.31, m/z 206 [(M - Boc) + H]⁺. ¹H NMR (500 MHz, CDCl₃) δ 1.50 (s, 9 H), 2.45 (br s, 2 H), 3.59 (br s, 2 H), 3.90 (d, $J = 1.4$ Hz, 3 H), 4.04 (br s, 2 H), 5.76 (br s, 1 H), 6.79–6.88 (m, 2 H).

tert-Butyl 4-(2,3-Difluoro-6-methoxyphenyl)-3,6-dihydropyridine-1(2H)-carboxylate (6g). Starting from 2-bromo-3,4-difluoroanisole (0.18 g, 0.81 mmol) and **5** (0.25 g, 0.81 mmol), compound **6g** (0.5 g, quant yield) was obtained as a colorless oil. C₁₇H₂₁F₂NO₃. LCMS: Rt 3.17, m/z 206 [(M - Boc) + H]⁺.

tert-Butyl 4-(2,4-Difluoro-6-methoxyphenyl)-3,6-dihydropyridine-1(2H)-carboxylate (6h). Step 1: methyl iodide (0.60 mL, 9.57 mmol) was added to a solution of 2-bromo-3,5-difluorophenol (1.0 g, 4.78 mmol) and K₂CO₃ (1.32 g, 9.57 mmol) in DMF (10 mL). The mixture was stirred under microwave irradiation at 150 °C for 10 min, and after cooling to rt it was then treated with H₂O and extracted with EtOAc. The organic layer was separated, dried (Na₂SO₄), and filtered, and the solvent was evaporated *in vacuo* to give 2-bromo-1,5-difluoro-3-methoxybenzene (1.05 g, quant yield) as an oil that solidified upon standing. The compound was used as such in the next reaction step. C₇H₃BrF₂O. GCMS: Rt 2.40, m/z 222 [M]⁺. Step 2: starting from 2-bromo-1,5-difluoro-3-methoxybenzene (1.05 g, 4.78 mmol) and **5** (1.5 g, 4.78 mmol), compound **6h** (1.13 g, 73%) was obtained as a colorless oil that solidified on standing. C₁₇H₂₁F₂NO₃. LCMS: Rt 3.87, m/z 311

[(M - Me) + H]⁺. ¹H NMR (500 MHz, CDCl₃) δ 1.50 (s, 9 H), 2.32 (br s, 2 H), 3.60 (br s, 2 H), 3.78 (s, 3 H), 4.04 (br s, 2 H), 5.63 (br s, 1 H), 6.40–6.48 (m, 2 H).

4-(3,6-Difluoro-2-methoxyphenyl)piperidine (7f). A solution of **6f** (0.23 g, 0.71 mmol) in EtOH (15 mL) was hydrogenated in a H-Cube reactor (1 mL/min, Pd(OH)₂ 20% cartridge, full H₂ mode, 80 °C). The solvent was evaporated *in vacuo*. The crude material obtained was used in the next reaction step without further purification. C₁₇H₂₃F₂NO₃. LCMS: Rt 3.29, *m/z* 655 [(MM + H)]⁺. ¹H NMR (400 MHz, CDCl₃) δ 1.49 (s, 9 H), 1.61 (br d, *J* = 13.2 Hz, 2 H), 2.05 (qd, *J* = 12.6, 3.5 Hz, 2 H), 2.77 (br t, *J* = 11.3, 11.3 Hz, 2 H), 3.19 (tt, *J* = 12.4, 3.5 Hz, 1 H), 3.91 (d, *J* = 1.8 Hz, 3 H), 4.23 (br s, 2 H), 6.70 (td, *J* = 9.6, 3.9 Hz, 1 H), 6.90 (ddd, *J* = 10.8, 9.1, 4.9 Hz, 1 H). The residue was dissolved in MeOH, HCl (7 M in *i*PrOH, 2 mL) was added, and the mixture was stirred at rt for 1.5 h. Then, the reaction mixture was diluted with Na₂CO₃ (aqueous saturated solution) and extracted with DCM. The organic phase was separated and dried (Na₂SO₄), and the solvent was evaporated *in vacuo* to yield compound **7f** (0.12 g, 85%) as a white solid. C₁₂H₁₅F₂NO. LCMS: Rt 1.19, *m/z* 228 [(M + H)]⁺. ¹H NMR (400 MHz, CDCl₃) δ 1.85 (br d, *J* = 13.9 Hz, 2 H), 2.65 (qd, *J* = 13.3, 3.7 Hz, 2 H), 2.98 (td, *J* = 13.1, 2.5 Hz, 2 H), 3.27 (tt, *J* = 12.4, 3.2 Hz, 1 H), 3.63 (br d, *J* = 12.5 Hz, 2 H), 4.01 (d, *J* = 2.5 Hz, 3 H), 6.71 (td, *J* = 9.4, 3.8 Hz, 1 H), 6.94 (ddd, *J* = 11.0, 9.2, 5.2 Hz, 1 H), 7.27 (br s, 1 H).

In a similar manner, compounds **7b–e,g,h** were also synthesized.

4-(5-Fluoro-2-methoxyphenyl)piperidine(7b). Starting from **6b** (3.4 g, 7.41 mmol) after reduction of the double bond and deprotection of the *N*-Boc protecting group, compound **7b** (0.76 g, 44% yield) was obtained as white solid. C₁₂H₁₆FNO. LCMS: Rt 1.85, *m/z* 210 [(M + H)]⁺.

4-(2-Fluoro-6-methoxyphenyl)piperidine (7c). Starting from **6c** (2 g, 6.5 mmol) after reduction of the double bond and deprotection of the *N*-Boc protecting group, compound **7c** (1.0 g, 73% yield) was obtained as a white solid. C₁₂H₁₆FNO. LCMS: Rt 0.55, *m/z* 210 [(M + H)]⁺.

4-(3-Fluoro-2-methoxyphenyl)piperidine Hydrochloride (7d). Starting from **6d** (1.13 g, 3.67 mmol), the double bond was reduced as previously described. The crude material was then dissolved in HCl (7 M in *i*PrOH, 8.5 mL), and the reaction mixture was stirred for 1.5 h. The solvent was then evaporated to give **7d** as the hydrochloride salt (0.9 g, quant yield) as a white solid. C₁₂H₁₆FNO. LCMS: Rt 0.74, *m/z* 210 [(M + H)]⁺. ¹H NMR (400 MHz, DMSO-*d*₆) δ 1.81 (qd, *J* = 12.5, 4.2 Hz, 2 H), 1.90 (br d, *J* = 11.8 Hz, 2 H), 2.79 (tt, *J* = 11.8, 3.8 Hz, 1 H), 2.87–3.02 (m, 2 H), 3.32 (br d, *J* = 12.9 Hz, 2 H), 3.81 (s, 3 H), 6.99 (dd, *J* = 8.6, 1.8 Hz, 1 H), 7.06 (dd, *J* = 12.9, 2.1 Hz, 1 H), 7.12 (t, *J* = 8.8 Hz, 1 H), 8.96 (br s, 1 H), 9.06 (br s, 1 H).

4-(3,4-Difluoro-2-methoxyphenyl)piperidine (7e). Starting from **6e** (0.54 g, 1.66 mmol) after reduction of the double bond and deprotection of the *N*-Boc protecting group, derivative **7e** (0.38 g, quant yield) was obtained as a white solid. C₁₂H₁₅F₂NO. LCMS: Rt 1.35, *m/z* 228 [(M + H)]⁺.

4-(2,3-Difluoro-6-methoxyphenyl)piperidine (7g). Starting from **6g** (0.13 g, 0.41 mmol) after reduction of the double bond and deprotection of the *N*-Boc protecting group, compound **7g** (0.09 g, quant yield) was obtained as white solid. C₁₂H₁₅F₂NO. LCMS: Rt 0.85, *m/z* 228 [(M + H)]⁺.

4-(2,4-Difluoro-6-methoxyphenyl)piperidine (7h). Starting from compound **6h** (0.726 g, 2.23 mmol) after reduction of the double bond and deprotection of the *N*-Boc protecting group, compound **7h** (0.525 g, quant yield) was obtained as a yellow oil. C₁₂H₁₅F₂NO. LCMS: Rt 0.67, *m/z* 228 [(M + H)]⁺. ¹H NMR (500 MHz, CDCl₃) δ 1.60 (br d, *J* = 13.3 Hz, 2 H), 2.08–2.21 (m, 2 H), 2.53 (br s, 1 H), 2.71–2.80 (m, 2 H), 3.13–3.26 (m, 3 H), 3.81 (s, 3 H), 6.34–6.46 (m, 2 H).

2-Bromo-4-[4-(3-fluoro-2-methoxyphenyl)piperidin-1-yl]pyridine-3-carbonitrile (10d). To a suspension of NaH (60% in mineral oil, 0.13 g, 3.27 mmol) in DMF (10 mL) was added **7d** at 0 °C. The reaction mixture was stirred at 0 °C for 5 min, and 2,4-dibromopyridine-3-carbonitrile (8,²⁸ 0.86 g, 3.27 mmol) was added. The reaction was allowed to reach rt and stirred for 1 h. Then the

reaction mixture was quenched with water and extracted with DCM. The organic layer was separated, dried (Na₂SO₄), and filtered, and the solvent was evaporated. The solid compound obtained was then washed with diisopropyl ether to afford compound **10d** that was used as such in the next reaction step (0.943 g, 74%). C₁₈H₁₇BrFN₃O. LCMS: Rt 3.34, *m/z* 390 [(M + H)]⁺.

2,3-Dichloro-4-[4-(5-fluoro-2-methoxyphenyl)piperidin-1-yl]pyridine (11b). To a suspension of **7b** (0.79 g, 3.78 mmol) and 2,3-dichloro-4-iodopyridine (**9**, 0.87 g, 3.15 mmol) in MeCN (8 mL) was added diisopropylethylamine (1.37 mL, 7.89 mmol). The mixture was heated at 110 °C overnight. Then the solvent was evaporated and the crude mixture was purified by column chromatography (silica gel, DCM in heptane 80/20), and the desired fractions were collected and concentrated *in vacuo*, yielding compound **11b** (0.55 g, 48.5%) as a white solid. C₁₇H₁₇Cl₂FN₂O. LCMS: Rt 3.30, *m/z* 355 [(M + H)]⁺.

4-[4-(3-Fluoro-2-methoxyphenyl)piperidin-1-yl]-2-hydrazinopyridine-3-carbonitrile (12d). A mixture of **10d** (0.94 g, 2.41 mmol) and hydrazine (0.59 mL, 12.1 mmol) in THF (10 mL) was heated in a microwave oven for 15 min at 160 °C. Then the solvent was evaporated to dryness, the residue was taken up with a solution of NH₃ in MeOH and then treated with Na₂CO₃ (aqueous saturated solution), and the mixture was extracted with DCM. The organic layer was separated, dried (Na₂SO₄), and filtered, and the solvent was evaporated. The solid material obtained was then washed with Et₂O, yielding compound **12d** that was used without further purification in the next reaction step (0.62 g, 75%). C₂₀H₂₀FN₅O. LCMS: Rt 3.02, *m/z* 342 [(M + H)]⁺.

3-Chloro-4-[4-(5-fluoro-2-methoxyphenyl)piperidin-1-yl]-2-hydrazinopyridine (13b). Compound **13b** was synthesized following a similar procedure as described for **12d**. Starting from **11b** (0.55 g, 1.53 mmol), compound **13b** was obtained (0.52 g, 92%) as a yellow oil. C₁₇H₂₀ClFN₄O. LCMS: Rt 2.95, *m/z* 351 [(M + H)]⁺.

***N'*-[3-Cyano-4-[4-(3-fluoro-2-methoxyphenyl)piperidin-1-yl]pyridin-2-yl]-3,3,3-trifluoropropylhydrazide (14d).** To a solution of compound **12d** (0.10 g, 0.293 mmol) and Et₃N (0.061 mL, 0.44 mmol) in DCM was added 3,3,3-trifluoropropionyl chloride (0.044 mL, 0.352 mmol) portionwise at 0 °C. The reaction was stirred for 10 min at rt. Then Na₂CO₃ (aqueous saturated solution) was added; the organic layer was separated, dried (Na₂SO₄), and filtered; and the solvent was evaporated in vacuum to give compound **14d**, which was used as such in the next reaction step (0.13 g, quant yield).

3,3,3-Trifluoropropionic Acid *N*-[3-Chloro-4-(5-fluoro-2-methoxyphenyl)-3,4,5,6-tetrahydro-2H-[1,4]bipyridinyl-2-yl]hydrazide (15b). Compound **15b** was synthesized following a similar procedure as described for **14d**. Starting from **13b** (0.53 g, 1.51 mmol), compound **15b** was obtained (0.35 g, 54%) as a yellow oil. C₂₀H₂₁ClF₄N₄O₂. LCMS: Rt 2.99, *m/z* 461 [(M + H)]⁺.

7-[4-(3-Fluoro-2-methoxyphenyl)piperidin-1-yl]-3-(2,2,2-trifluoroethyl)[1,2,4]triazolo[4,3-*a*]pyridine-8-carbonitrile (16d). A solution of **14d** (0.133 g, 0.295 mmol) and POCl₃ (0.055 mL, 0.59 mmol) in MeCN was heated in a microwave oven for 5 min at 150 °C. Then Na₂CO₃ (aqueous saturated solution) and DCM were added. The organic layer was separated and dried (Na₂SO₄), and the solvent was evaporated. The residue was purified by column chromatography (silica gel, EtOAc in DCM 10/90 to 80/20). The solid compound obtained was then washed with diisopropyl ether to yield compound **16d** as a sticky solid (0.073 g, 57%). C₂₁H₁₉ClF₄N₅O. LCMS: Rt 4.19, *m/z* 434 [(M + H)]⁺. ¹H NMR (500 MHz, DMSO-*d*₆) δ 1.80 (qd, *J* = 12.4, 3.2 Hz, 2 H), 1.87 (br d, *J* = 10.7 Hz, 2 H), 3.29 (tt, *J* = 11.8, 3.8 Hz, 1 H), 3.39–3.48 (m, 2 H), 3.87 (d, *J* = 1.2 Hz, 3 H), 4.37 (br d, *J* = 12.7 Hz, 2 H), 4.40 (q, *J* = 10.7 Hz, 2 H), 7.04–7.16 (m, 4 H), 8.52 (d, *J* = 7.8 Hz, 1 H).

8-Chloro-7-[4-(5-fluoro-2-methoxyphenyl)-1-piperidinyl]-3-(2,2,2-trifluoroethyl)-1,2,4-triazolo[4,3-*a*]pyridine (17b). Compound **17b** was synthesized following a similar procedure as described for **16d**. Starting from **15b** (0.35 g, 0.77 mmol), compound **17b** was obtained as a white solid (0.11 g, 33%); mp 259 °C. C₂₀H₁₉ClF₄N₄O. LCMS: Rt 3.87, *m/z* 443 [(M + H)]⁺. ¹H NMR (500 MHz, CDCl₃) δ 1.89 (qd, *J* = 12.4, 3.8 Hz, 2 H), 1.94–2.00 (m, 2 H), 3.08 (td, *J* = 11.8, 2.3 Hz, 2 H), 3.15 (tt, *J* = 11.9, 3.4 Hz, 1 H), 3.73–3.79 (m, 2 H), 3.83 (s, 3 H), 4.02 (q, *J* = 9.8 Hz, 2 H), 6.80 (dd, *J* = 9.0, 4.6 Hz, 1

H), 6.85 (d, $J = 7.5$ Hz, 1 H), 6.86–6.91 (m, 1 H), 6.97 (dd, $J = 9.5$, 3.2 Hz, 1 H), 7.86 (d, $J = 7.2$ Hz, 1 H).

8-Chloro-3-(cyclopropylmethyl)-7-[4-(3,6-difluoro-2-methoxyphenyl)-1-piperidinyl]-1,2,4-triazolo[4,3-*a*]pyridine (20f). To a mixture of 8-chloro-3-(cyclopropylmethyl)-7-iodo[1,2,4]triazolo[4,3-*a*]pyridine²⁹ (**18**, 0.25 g, 0.75 mmol) and **7f** (0.22 g, 0.97 mmol) in toluene (2.5 mL) were added Pd(OAc)₂ (0.008 g, 0.04 mmol), (±)BINAP (0.046 g, 0.07 mmol), and Cs₂CO₃ (0.37 g, 1.12 mmol). The reaction mixture was heated at 125 °C overnight. Then DCM was added, the solid was filtered off, the filtrate solvent evaporated *in vacuo*, and the crude material purified by column chromatography (MeOH in DCM 0/100 to 5/95). The desired fractions were collected, the solvent was evaporated *in vacuo*, and the solid material obtained was then washed with Et₂O to yield compound **20f** as an off-white solid (0.19 g, 59.2%); mp 163.2 °C. C₂₂H₂₃ClF₂N₄O. LCMS: Rt 2.43, m/z 443 [(M + H)⁺]. ¹H NMR (500 MHz, CDCl₃) δ 0.20–0.38 (m, 2 H), 0.47–0.67 (m, 2 H), 1.13–1.20 (m, 1 H), 1.78 (br d, $J = 12.4$ Hz, 2 H), 2.41 (qd, $J = 12.5$, 2.7 Hz, 2 H), 3.01 (t, $J = 12.1$ Hz, 2 H), 3.05 (d, $J = 6.9$ Hz, 2 H), 3.25 (tt, $J = 12.5$, 3.4 Hz, 1 H), 3.72 (br d, $J = 11.8$ Hz, 2 H), 3.95 (d, $J = 1.7$ Hz, 3 H), 6.74 (td, $J = 9.2$, 4.0 Hz, 1 H), 6.76 (d, $J = 7.5$ Hz, 1 H), 6.93 (ddd, $J = 10.5$, 9.2, 5.1 Hz, 1 H), 7.84 (d, $J = 7.5$ Hz, 1 H).

8-Chloro-3-(cyclopropylmethyl)-7-[4-(2-methoxyphenyl)-1-piperidinyl]-1,2,4-triazolo[4,3-*a*]pyridine (20a). Compound **20a** was synthesized following the same procedure as described for compound **20f**. Starting from intermediates **18** (0.15 g, 0.45 mmol) and 4-(2-methoxyphenyl)piperidine²⁶ (**7a**, 0.1 g, 0.54 mmol), compound **20a** was obtained as a foam (0.056 g, 29.5%). C₂₂H₂₅ClN₄O. LCMS: Rt 3.38, m/z 397 [(M + H)⁺]. ¹H NMR (400 MHz, CDCl₃) δ 0.25–0.39 (m, 2 H), 0.54–0.67 (m, 2 H), 1.10–1.23 (m, 1 H), 1.87–2.03 (m, 4 H), 3.00–3.09 (m, 4 H), 3.11–3.21 (m, 1 H), 3.71 (br d, $J = 12.5$ Hz, 2 H), 3.86 (s, 3 H), 6.77 (d, $J = 7.4$ Hz, 1 H), 6.89 (br d, $J = 8.1$ Hz, 1 H), 6.97 (br t, $J = 7.4$, 7.4 Hz, 1 H), 7.19–7.24 (m, 1 H), 7.25–7.29 (m, 1 H), 7.84 (d, $J = 7.6$ Hz, 1 H).

8-Chloro-3-(cyclopropylmethyl)-7-[4-(5-fluoro-2-methoxyphenyl)-1-piperidinyl]-1,2,4-triazolo[4,3-*a*]pyridine (20b). A suspension of compounds **18** (0.10 g, 0.30 mmol), **7b** (0.13 g, 0.60 mmol), and NaHCO₃ (0.061 g, 0.75 mmol) in MeCN (1 mL) was heated in a pressure tube (Q-Tube) at 180 °C overnight. Then the mixture was diluted with DCM and HCl (2 N in H₂O), the organic layer separated and dried (Na₂SO₄), and the solvent evaporated *in vacuo*. The crude material was purified by column chromatography (EtOAc in DCM 0/100 to 100/0), the desired fractions were collected, and the solvent was evaporated *in vacuo*. The solid compound obtained was then washed with diisopropyl ether to yield compound **20b** as an off-white solid (0.06 g, 49%); mp >300 °C. C₂₂H₂₄ClFN₄O. LCMS: Rt 3.43, m/z 415 [(M + H)⁺]. ¹H NMR (500 MHz, CDCl₃) δ 0.27–0.38 (m, 2 H), 0.55–0.67 (m, 2 H), 1.13–1.20 (m, 1 H), 1.89 (qd, $J = 12.1$, 3.8 Hz, 2 H), 1.93–1.99 (m, 2 H), 3.00–3.07 (m, 2 H), 3.05 (d, $J = 6.6$ Hz, 2 H), 3.14 (tt, $J = 11.7$, 3.6 Hz, 1 H), 3.71 (br d, $J = 11.8$ Hz, 2 H), 3.83 (s, 3 H), 6.76 (d, $J = 7.5$ Hz, 1 H), 6.80 (dd, $J = 9.0$, 4.6 Hz, 1 H), 6.86–6.92 (m, 1 H), 6.97 (dd, $J = 9.5$, 3.2 Hz, 1 H), 7.84 (d, $J = 7.5$ Hz, 1 H).

8-Chloro-3-(cyclopropylmethyl)-7-[4-(2-fluoro-6-methoxyphenyl)-1-piperidinyl]-1,2,4-triazolo[4,3-*a*]pyridine (20c). Compound **20c** was synthesized following a similar procedure to that described for its analogue **20b**, changing the heating system from pressure tube to microwave irradiation (230 °C, 30 min). Thus, starting from intermediate **18** (0.10 g, 0.30 mmol) and intermediate **7c** (0.094 g, 0.45 mmol), the title compound **20c** was obtained as a foam (0.05 g, 38.5%). C₂₂H₂₄ClFN₄O. LCMS: Rt 4.72, m/z 415 [(M + H)⁺]. ¹H NMR (500 MHz, CDCl₃) δ 0.28–0.38 (m, 2 H), 0.56–0.66 (m, 2 H), 1.13–1.22 (m, 1 H), 1.71–1.78 (m, 2 H), 2.45 (qd, $J = 12.3$, 3.2 Hz, 2 H), 3.01 (br t, $J = 11.8$ Hz, 2 H), 3.05 (d, $J = 6.6$ Hz, 2 H), 3.31 (tt, $J = 12.3$, 3.5 Hz, 1 H), 3.72 (br d, $J = 11.8$ Hz, 2 H), 3.85 (s, 3 H), 6.66–6.72 (m, 2 H), 6.77 (d, $J = 7.5$ Hz, 1 H), 7.15 (td, $J = 8.3$, 6.5 Hz, 1 H), 7.83 (d, $J = 7.5$ Hz, 1 H).

8-Chloro-3-(cyclopropylmethyl)-7-[4-(3-fluoro-2-methoxyphenyl)-1-piperidinyl]-1,2,4-triazolo[4,3-*a*]pyridine (20d). Compound **20d** was synthesized following the same procedure described for

compound **20f**. Starting from intermediates **18** (0.10 g, 0.30 mmol) and **7d** (0.075 g, 0.36 mmol), the title compound **20d** was obtained as an off-white solid (0.025 g, 19.5%); mp 168.3 °C. C₂₂H₂₄ClFN₄O. LCMS: Rt 3.40, m/z 415 [(M + H)⁺]. ¹H NMR (400 MHz, CDCl₃) δ 0.26–0.39 (m, 2 H), 0.54–0.68 (m, 2 H), 1.11–1.23 (m, 1 H), 1.86–2.04 (m, 4 H), 2.98–3.10 (m, 4 H), 3.11–3.21 (m, 1 H), 3.67–3.75 (m, 2 H), 3.95 (d, $J = 1.8$ Hz, 3 H), 6.77 (d, $J = 7.4$ Hz, 1 H), 6.94–7.09 (m, 3 H), 7.85 (d, $J = 7.4$ Hz, 1 H).

8-Chloro-3-(cyclopropylmethyl)-7-[4-(3,4-difluoro-2-methoxyphenyl)-1-piperidinyl]-1,2,4-triazolo[4,3-*a*]pyridine (20e). Compound **20e** was synthesized following the same approach described for compound **20f**. Starting from intermediates **18** (0.15 g, 0.45 mmol) and **7e** (0.12 g, 0.54 mmol), compound **20e** was obtained as an off-white solid (0.042 g, 21%); mp 173.5 °C. C₂₂H₂₃ClF₂N₄O. LCMS: Rt 3.56, m/z 433 [(M + H)⁺]. ¹H NMR (400 MHz, CDCl₃) δ 0.26–0.39 (m, 2 H), 0.54–0.68 (m, 2 H), 1.11–1.23 (m, 1 H), 1.85–2.00 (m, 4 H), 2.97–3.13 (m, 5 H), 3.70 (br d, $J = 11.8$ Hz, 2 H), 4.00 (d, $J = 2.1$ Hz, 3 H), 6.75 (d, $J = 7.4$ Hz, 1 H), 6.83–6.92 (m, 1 H), 6.93–6.99 (m, 1 H), 7.84 (d, $J = 7.4$ Hz, 1 H).

8-Chloro-3-(cyclopropylmethyl)-7-[4-(2,3-difluoro-6-methoxyphenyl)-1-piperidinyl]-1,2,4-triazolo[4,3-*a*]pyridine (20g). Compound **20g** was synthesized following the same procedure described for compound **20f**. Starting from intermediates **18** (0.10 g, 0.30 mmol) and **7g** (0.08 g, 0.36 mmol), compound **20g** was obtained as an off-white solid (0.04 g, 27.6%); mp 208.5 °C. C₂₂H₂₃ClF₂N₄O. LCMS: Rt 3.48, m/z 433 [(M + H)⁺]. ¹H NMR (400 MHz, CDCl₃) δ 0.26–0.39 (m, 2 H), 0.54–0.68 (m, 2 H), 1.11–1.22 (m, 1 H), 1.71–1.80 (m, 2 H), 2.45 (qd, $J = 12.4$, 3.4 Hz, 2 H), 3.00 (br t, $J = 11.4$, 2 H), 3.05 (d, $J = 6.7$ Hz, 2 H), 3.30 (tt, $J = 12.4$, 3.5 Hz, 1 H), 3.67–3.75 (m, 2 H), 3.83 (s, 3 H), 6.52–6.61 (m, 1 H), 6.76 (d, $J = 7.6$ Hz, 1 H), 6.98 (q, $J = 9.2$ Hz, 1 H), 7.83 (d, $J = 7.6$ Hz, 1 H).

8-Chloro-3-(cyclopropylmethyl)-7-[4-(2,4-difluoro-6-methoxyphenyl)-1-piperidinyl]-1,2,4-triazolo[4,3-*a*]pyridine (20h). Compound **20h** was synthesized following the same procedure described for **20f**. Starting from intermediate **18** (0.10 g, 0.30 mmol) and **7h** (0.08 g, 0.36 mmol), compound **20h** was obtained as an off-white solid (0.05 g, 38%); mp 162.2 °C. C₂₂H₂₃ClF₂N₄O. LCMS: Rt 3.6, m/z 433 [(M + H)⁺]. ¹H NMR (500 MHz, CDCl₃) δ 0.28–0.38 (m, 2 H), 0.55–0.67 (m, 2 H), 1.12–1.21 (m, 1 H), 1.68–1.76 (m, 2 H), 2.40 (qd, $J = 12.3$, 3.3 Hz, 2 H), 2.98 (br t, $J = 11.7$ Hz, 2 H), 3.05 (d, $J = 6.6$ Hz, 2 H), 3.22 (tt, $J = 12.4$, 3.6 Hz, 1 H), 3.70 (br d, $J = 11.8$ Hz, 2 H), 3.84 (s, 3 H), 6.39–6.47 (m, 2 H), 6.76 (d, $J = 7.5$ Hz, 1 H), 7.83 (d, $J = 7.5$ Hz, 1 H).

3-(Cyclopropylmethyl)-7-[4-(3,6-difluoro-2-methoxyphenyl)-1-piperidinyl]-8-(trifluoromethyl)-1,2,4-triazolo[4,3-*a*]pyridine (21f). A mixture of 7-chloro-3-(cyclopropylmethyl)-8-(trifluoromethyl)[1,2,4]-triazolo[4,3-*a*]pyridine³⁰ (**19**, 0.30 g, 1.09 mmol), **7f** (0.37 g, 1.63 mmol), and diisopropylamine (0.38 mL, 2.18 mmol) in MeCN (3 mL) was heated under microwave irradiation at 190 °C for 20 min. Then the solvent was evaporated, and the crude residue was purified by column chromatography (EtOAc in DCM 0/100 to 100/0). The desired fractions were collected, and the solvent was evaporated *in vacuo*. The solid compound obtained was then washed with diisopropyl ether to yield compound **21f** as an off-white solid (0.25 g, 48.2%); mp 180.7 °C. C₂₃H₂₃F₃N₄O. LCMS: Rt 3.56, m/z 467 [(M + H)⁺]. ¹H NMR (500 MHz, CDCl₃) δ 0.28–0.38 (m, 2 H), 0.57–0.67 (m, 2 H), 1.11–1.20 (m, 1 H), 1.75 (dd, $J = 12.1$, 1.7 Hz, 2 H), 2.35 (qd, $J = 12.4$, 3.2 Hz, 2 H), 3.04 (d, $J = 6.6$ Hz, 2 H), 3.18 (br t, $J = 12.4$ Hz, 2 H), 3.27 (tt, $J = 12.4$, 3.6 Hz, 1 H), 3.62 (br d, $J = 12.7$ Hz, 2 H), 3.94 (d, $J = 2.0$ Hz, 3 H), 6.72 (ddd, $J = 9.8$, 9.3, 4.1 Hz, 1 H), 6.75 (d, $J = 7.5$ Hz, 1 H), 6.93 (ddd, $J = 10.8$, 9.2, 4.9 Hz, 1 H), 7.91 (d, $J = 7.5$ Hz, 1 H).

8-Chloro-3-(cyclopropylmethyl)-7-[4-(3-fluoro-2-methoxyphenyl)-1-piperidinyl]-1,2,4-triazolo[4,3-*a*]pyridine (21d). Compound **21d** was synthesized following the same procedure described for compound **21f**. Starting from intermediate **19** (0.10 g, 0.36 mmol) and **7d** (0.09 g, 0.44 mmol), compound **21d** was obtained as an off-white solid (0.045 g, 27.6%); mp 195.7 °C. C₂₂H₂₄F₄N₄O. LCMS: Rt 3.57, m/z 449 [(M + H)⁺]. ¹H NMR (500 MHz, CDCl₃) δ 0.28–0.39 (m, 2 H), 0.56–0.68 (m, 2 H), 1.08–1.20 (m, 1 H), 1.82–1.97 (m, 4

H), 3.05 (d, $J = 6.6$ Hz, 2 H), 3.10–3.18 (m, 1 H), 3.18–3.28 (m, 2 H), 3.60 (br d, $J = 13.0$ Hz, 2 H), 3.95 (d, $J = 1.7$ Hz, 3 H), 6.77 (d, $J = 7.8$ Hz, 1 H), 6.92–7.07 (m, 3 H), 7.93 (d, $J = 7.8$ Hz, 1 H).

2-[1-[8-Chloro-3-(cyclopropylmethyl)-1,2,4-triazolo[4,3-a]pyridin-7-yl]-4-piperidinyl]-3,6-difluorophenol (22f). To a solution of compound **20f** (0.05 g, 0.116 mmol) in DCM (0.5 mL) was added BBr_3 (0.231 mL, 0.231 mmol) dropwise at 0 °C. The reaction was stirred for 45 min at rt. The excess BBr_3 was quenched dropwise with MeOH (1 mL) at 0 °C, and then Na_2CO_3 (saturated aqueous solution) was added (to pH ~ 7). The organic layer was separated, dried (Na_2SO_4), and filtered, and the solvent was evaporated *in vacuo*. The residue was purified by column chromatography (silica gel, MeOH in DCM 0/100 to 6/94), the desired fractions were collected, and the solvent was evaporated *in vacuo*. The compound obtained was then treated with MeCN and then purified again by chromatography (same eluent as before) and then treated with Et_2O to yield finally the title compound **22f** (0.018 g, 38%) as a white solid; mp >300 °C. $\text{C}_{21}\text{H}_{21}\text{ClF}_2\text{N}_4\text{O}$. LCMS: Rt 2.02, m/z 419 [(M + H)]⁺. ^1H NMR (500 MHz, $\text{DMSO}-d_6$) δ 0.21–0.35 (m, 2 H), 0.45–0.56 (m, 2 H), 1.11–1.22 (m, 1 H), 1.70 (br d, $J = 10.7$ Hz, 2 H), 2.24–2.40 (m, 2 H), 2.98 (br t, $J = 11.8$ Hz, 2 H), 3.02 (d, $J = 6.9$ Hz, 2 H), 3.24 (tt, $J = 12.4, 3.3$ Hz, 1 H), 3.61 (br d, $J = 11.8$ Hz, 2 H), 6.63 (td, $J = 9.8, 3.9$ Hz, 1 H), 6.97 (d, $J = 7.5$ Hz, 1 H), 7.07 (td, $J = 9.7, 4.9$ Hz, 1 H), 8.38 (d, $J = 7.2$ Hz, 1 H), 9.99 (br s, 1 H).

2-[1-[8-Chloro-3-(cyclopropylmethyl)-1,2,4-triazolo[4,3-a]pyridin-7-yl]-4-piperidinyl]-4-fluorophenol (22b). Compound **22b** was synthesized following the same procedure described for compound **22f**. Starting from compound **20b** (0.238 g, 0.57 mmol), the title compound **22b** was obtained as an off-white solid (0.065 g, 28.2%); mp 256 °C. $\text{C}_{21}\text{H}_{22}\text{ClFN}_4\text{O}$. LCMS: Rt 3.04, m/z 401 [(M + H)]⁺. ^1H NMR (400 MHz, $\text{DMSO}-d_6$) δ 0.21–0.33 (m, 2 H), 0.44–0.57 (m, 2 H), 1.09–1.22 (m, 1 H), 1.72–1.83 (m, 2 H), 1.81–1.96 (m, 2 H), 2.89–3.13 (m, 5 H), 3.61 (br d, $J = 11.8$ Hz, 2 H), 6.73–6.91 (m, 2 H), 6.91–6.99 (m, 1 H), 6.98 (d, $J = 7.6$ Hz, 1 H), 8.38 (d, $J = 7.4$ Hz, 1 H), 9.40 (s, 1 H).

2-[1-[8-Chloro-3-(cyclopropylmethyl)-1,2,4-triazolo[4,3-a]pyridin-7-yl]-4-piperidinyl]-3-fluorophenol (22c). Compound **22c** was synthesized following the same procedure described for compound **22f**. Starting from compound **20c** (0.124 g, 0.29 mmol), the title compound **22c** was obtained as an off-white solid (0.034 g, 28.3%); mp 242.6 °C. $\text{C}_{21}\text{H}_{22}\text{ClFN}_4\text{O}$. LCMS: Rt 2.76, m/z 401 [(M + H)]⁺. ^1H NMR (500 MHz, $\text{DMSO}-d_6$) δ 0.21–0.34 (m, 2 H), 0.45–0.56 (m, 2 H), 1.05–1.21 (m, 1 H), 1.67 (br d, $J = 10.7$ Hz, 2 H), 2.25–2.35 (m, 2 H), 2.97 (br t, $J = 11.7$ Hz, 2 H), 3.02 (d, $J = 6.6$ Hz, 2 H), 3.22 (tt, $J = 12.3, 3.3$ Hz, 1 H), 3.60 (br d, $J = 11.8$ Hz, 2 H), 6.56 (dd, $J = 10.4, 8.7$ Hz, 1 H), 6.67 (d, $J = 8.1$ Hz, 1 H), 6.97 (d, $J = 7.2$ Hz, 1 H), 6.99–7.07 (m, 1 H), 8.39 (d, $J = 7.5$ Hz, 1 H), 9.96 (br s, 1 H).

2-[1-[8-Chloro-3-(cyclopropylmethyl)-1,2,4-triazolo[4,3-a]pyridin-7-yl]-4-piperidinyl]-3,4-difluorophenol (22g). Compound **22g** was synthesized following the same synthetic procedure described for compound **22f**. Starting from **20g** (0.142 g, 0.33 mmol), the title compound **22g** was obtained (0.016 g, 11.6%) as an off-white solid; mp >300 °C. $\text{C}_{21}\text{H}_{21}\text{ClF}_2\text{N}_4\text{O}$. LCMS: Rt 2.85, m/z 419 [(M + H)]⁺. ^1H NMR (500 MHz, $\text{DMSO}-d_6$) δ 0.21–0.33 (m, 2 H), 0.44–0.56 (m, 2 H), 1.12–1.21 (m, 1 H), 1.71 (br d, $J = 10.7$ Hz, 2 H), 2.18–2.36 (m, 2 H), 2.98 (br t, $J = 11.7$ Hz, 2 H), 3.02 (d, $J = 6.6$ Hz, 2 H), 3.19–3.27 (m, 1 H), 3.61 (br d, $J = 11.8$ Hz, 2 H), 6.60 (dd, $J = 9.0, 2.9$ Hz, 1 H), 6.98 (d, $J = 7.5$ Hz, 1 H), 7.04 (q, $J = 9.5$ Hz, 1 H), 8.39 (d, $J = 7.5$ Hz, 1 H), 10.10 (br s, 1 H).

2-[1-[8-Chloro-3-(cyclopropylmethyl)-1,2,4-triazolo[4,3-a]pyridin-7-yl]-4-piperidinyl]-3,5-difluorophenol (22h). Compound **22h** was synthesized following the same procedure described for **22f**. Starting from **20h**, the title compound **22h** (0.129 g, 0.29 mmol) was obtained as an off-white solid (0.014 g, 11.2%); mp >300 °C. $\text{C}_{21}\text{H}_{21}\text{ClF}_2\text{N}_4\text{O}$. LCMS: Rt 2.97, m/z 419 [(M + H)]⁺. ^1H NMR (500 MHz, $\text{DMSO}-d_6$) δ 0.22–0.32 (m, 2 H), 0.45–0.56 (m, 2 H), 1.12–1.21 (m, 1 H), 1.66 (br d, $J = 10.7$ Hz, 2 H), 2.18–2.34 (m, 2 H), 2.96 (br t, $J = 11.7$ Hz, 2 H), 3.02 (d, $J = 6.9$ Hz, 2 H), 3.10–3.20 (m, 1 H), 3.59 (br d, $J = 11.8$ Hz, 2 H), 6.48 (br d, $J = 10.4$ Hz, 1 H),

6.51–6.61 (m, 1 H), 6.96 (d, $J = 7.5$ Hz, 1 H), 8.37 (d, $J = 7.5$ Hz, 1 H), 10.44 (br s, 1 H).

2-[1-[3-(Cyclopropylmethyl)-8-(trifluoromethyl)-1,2,4-triazolo[4,3-a]pyridin-7-yl]-4-piperidinyl]-3,6-difluorophenol (23f). Compound **23f** was synthesized following the same procedure reported for **22f**. Starting from compound **21f** (0.15 g, 0.32 mmol) after deprotection with BBr_3 , compound **23f** was obtained (0.01 g, 8.9%) as a white solid; mp >300 °C. $\text{C}_{22}\text{H}_{21}\text{F}_5\text{N}_4\text{O}$. LCMS: Rt 2.92, m/z 453 [(M + H)]⁺. ^1H NMR (500 MHz, $\text{DMSO}-d_6$) δ 0.21–0.35 (m, 2 H), 0.42–0.59 (m, 2 H), 1.11–1.21 (m, 1 H), 1.67 (br d, $J = 11.0$ Hz, 2 H), 2.15–2.34 (m, 2 H), 3.00 (d, $J = 6.9$ Hz, 2 H), 3.17 (br t, $J = 12.1$ Hz, 2 H), 3.53 (br d, $J = 12.4$ Hz, 2 H), 6.60 (td, $J = 9.5, 3.3$ Hz, 1 H), 7.00 (d, $J = 7.8$ Hz, 1 H), 7.05 (td, $J = 9.6, 5.1$ Hz, 1 H), 8.47 (d, $J = 7.5$ Hz, 1 H), 9.96 (br s, 1 H).

Radiochemistry. Carbon-11 was produced *via* a [$^{14}\text{N}(\text{p},\alpha)^{11}\text{C}$] nuclear reaction. The target gas, which is a mixture of N_2 (95%) and H_2 (5%) was irradiated using 18-MeV protons at a beam current of 25 μA . The irradiation was done for about 30 min to yield [^{11}C]methane ([^{11}C]CH₄). [^{11}C]CH₄ was then reacted with vaporized I_2 at 650 °C to convert it to [^{11}C]methyl iodide ([^{11}C]MeI). The resulting volatile [^{11}C]MeI was bubbled with a flow of helium through a solution of radiolabeling precursor **22b** (for [^{11}C]20b), **22c** (for [^{11}C]20c), **22f** (for [^{11}C]20f), **22g** (for [^{11}C]20g), **22h** (for [^{11}C]20h), **23f** (for [^{11}C]21f) (0.2 mg), and Cs_2CO_3 (1–3 mg) in anhydrous DMF (0.2 mL). When the amount of radioactivity in the reaction vial had stabilized, the reaction mixture was heated at 90 °C for 3 min. After dilution with water (0.7 mL), the crude reaction mixture was injected onto an HPLC system consisting of a semipreparative XBridge column (C_{18} , 5 μm ; 4.6 mm \times 150 mm; Waters, Milford, MA, USA) that was eluted with a mixture of 0.05 M sodium acetate buffer (pH 5.5) and EtOH (50:50 v/v) at a flow rate of 1 mL/min. The radiolabeled product was collected between 12 and 16 min (small difference in retention time for the different tracers). The collected peak corresponding to the desired radioligand was then diluted with saline (Mini Plasco, Braun, Melsungen, Germany) to obtain a final ethanol concentration of 10%, and the solution was sterile filtered through 0.22 μm membrane filter (Millex-GV, Millipore, Ireland). Quality control was performed on an analytical HPLC system consisting of an XBridge C_{18} 3.5 μm column (3 mm \times 100 mm; Waters) eluted with a mixture of 0.05 M NaOAc buffer (pH 5.5) and MeCN (55:45 v/v) at a flow rate of 0.8 mL/min (Rt = 4–7 min, small difference in retention time for the different tracers). UV detection was performed at 254 nm. The six carbon-11 labeled tracers were synthesized with a radiochemical yield of 35–74% (relative to starting radioactivity of [^{11}C]MeI, nondecay corrected, $n > 3$ for each tracer). The radiochemical purity as examined using the above-described analytical HPLC system was $>96\%$, and the average specific radioactivity was found to be in the range 54–239 GBq/ μmol at end of synthesis (EOS) ($n > 3$ for each tracer).

Biology. Membrane Preparation. CHO cells expressing the human mGlu2 receptor were grown until 80% confluence, washed in ice-cold phosphate-buffered saline, and stored at -20 °C until membrane preparation. After thawing, cells were suspended in 50 mM Tris-HCl, pH 7.4, and collected through centrifugation for 10 min at 23,500g at 4 °C. Cells were lysed in 5 mM hypotonic Tris-HCl, pH 7.4, and after recentrifugation for 20 min at 30,000g at 4 °C, the pellet was homogenized with an Ultra Turrax homogenizer in 50 mM Tris-HCl, pH 7.4. Protein concentrations were measured by the Bio-Rad protein assay using bovine serum albumin as standard. [^{35}S]GTP γS binding assay. For [^{35}S]GTP γS measurements, compound and glutamate were diluted in buffer containing 10 mM HEPES acid, 10 mM HEPES salt, pH 7.4, containing 100 mM NaCl, 3 mM MgCl_2 , and 10 μM GDP. Membranes were thawed on ice and diluted in the same buffer, supplemented with 14 $\mu\text{g}/\text{mL}$ saponin (final assay concentration of 2 $\mu\text{g}/\text{mL}$ saponin). Final assay mixtures contained 7 μg of membrane protein and were preincubated with compound alone (determination of agonist effects) or together with an EC_{20} concentration (4 μM) of glutamate (determination of PAM effects) for 30 min at 30 °C. [^{35}S]GTP γS was added at a final concentration of 0.1 nM and incubated for another 30 min at 30 °C. Reactions were terminated by rapid filtration through Unifilter-96 GF/B filter plates

(PerkinElmer) using a Unifilter-96 Harvester (PerkinElmer). Filters were washed three times with ice-cold 10 mM NaH_2PO_4 /10 mM Na_2HPO_4 , pH 7.4, and filter-bound radioactivity was counted in a Topcount Microplate Scintillation and Luminescence Counter from PerkinElmer. **Binding Assay.** After thawing, membranes from hmGlu2-CHO cells were homogenized using an Ultra Turrax homogenizer and suspended in ice-cold binding buffer containing 50 mM Tris-HCl (pH 7.4), 10 mM MgCl_2 , and 2 mM CaCl_2 . Displacement studies were performed using 10 nM of radioligand [^3H]2, JNJ-40068782. Assay mixtures were incubated for 60 min at room temperature in a volume of 0.5 mL containing 75 μg hmGlu2 CHO membrane protein. Nonspecific binding (about 30% of total binding) was estimated in the presence of 10 μM JNJ-40264796, a structurally-related molecule. Filtration was performed using Unifilter-96 GF/C filters presoaked in 0.1% PEI and a 40-well manifold or 96-well Brandell harvester 96. After the addition of scintillation liquid, radioactivity on the filters was counted in a Microplate Scintillation and Luminescence Counter or Liquid Scintillation Analyzer from Perkin-Elmer.

Biodistribution Studies and Radiometabolite Analysis. Quantification of radioactivity measurements in samples of biodistribution studies and radiometabolite analysis was done using an automated gamma counter equipped with a 3-in. NaI(Tl) well crystal coupled to a multichannel analyzer (Wallac 1480 Wizard, Wallac, Turku, Finland). The results were corrected for background radiation, physical decay, and counter dead time. All animal experiments were conducted with the approval of the institutional ethical committee for conduct of experiments on animals. **Biodistribution Studies.** Biodistribution studies were carried out in healthy male Wistar rats (body weight 200–450 g) at 2, 30, and 60 min pi ($n = 3$ /time point). Rats were injected with about 22 MBq of the tracer *via* tail vein under anesthesia (2.5% isoflurane in O_2 at 1 L/min flow rate) and sacrificed by decapitation at the above specified time points. Blood and major organs were collected in tared tubes and weighed. The radioactivity in blood, organs, and other body parts was measured using an automated gamma counter. For calculation of total radioactivity in blood, blood mass was assumed to be 7% of the body mass. **Plasma radiometabolite analysis.** After iv administration of about 74 MBq of the radioligand *via* tail vein under anesthesia (2.5% isoflurane in O_2 at 1 L/min flow rate), rats were sacrificed by decapitation at 30 min pi ($n = 2$ for [^{11}C]20b, [^{11}C]20g, [^{11}C]20h; $n = 3$ for [^{11}C]20f). Blood was collected in heparin containing tubes (4.5 mL LH PST tubes; BD vacutainer, BD, Franklin Lakes, NJ, USA) and stored on ice. Next, the blood was centrifuged for 5 min at 3000 rpm to separate the plasma. Plasma (0.5 mL) was spiked with 10 μg of the authentic nonradioactive compound. Plasma was then analyzed with HPLC (Chromolith C_{18} , 3 mm \times 100 mm, Merck) eluted with gradient mixtures of 0.05 M sodium acetate (pH 5.5) (A) and MeCN (B): 0–4 min: 0% B, flow rate 0.5 mL/min; 4–9 min: linear gradient 0% B to 90% B, flow rate 1 mL/min; 9–12 min: 90% B flow rate 1 mL/min; 12–20 min: linear gradient 90% B to 0% B, flow rate of 0.5 mL/min. After passing through an in-line UV detector (254 nm), the HPLC eluate was collected as 1 mL fractions. The radioactivity in all fractions was measured using an automated gamma counter. **Perfused brain radiometabolite analysis.** After administration of about 74 MBq of the radioligand *via* tail vein under anesthesia (2.5% isoflurane in O_2 at 1 L/min flow rate), rats ($n = 1$ for [^{11}C]20b, [^{11}C]20g, [^{11}C]20h; $n = 2$ for [^{11}C]20f) were sacrificed at 30 min pi by administering an overdose of Nembutal (CEVA Santé Animale, 200 mg/kg intraperitoneal). When breathing had stopped, the rats were perfused with saline (Mini Plasco, Braun, Melsungen, Germany) until the liver turned pale. Brain was isolated, and cerebrum and cerebellum were separated and homogenized in 3 and 2 mL of MeCN, respectively, for about 2 min. A volume of 1 mL of this homogenate was diluted with an equal volume of water, and a part of this homogenate was filtered through a 0.22 μm filter (Millipore, Bedford, USA). About 0.5 mL of the filtrate was diluted with 0.1 mL of water and spiked with 10 μg of authentic nonradioactive compound. The cerebrum/cerebellum homogenate extracts were then injected onto an HPLC system consisting of an analytical XBridge column (C_{18} , 3.5 μM , 3 mm \times 100

mm, Waters) eluted with a mixture of 0.05 M sodium acetate (pH 5.5) and MeCN (60:40 v/v) at a flow rate of 0.8 mL/min. The HPLC eluate was collected as 1-mL fractions after passing through the UV detector (254 nm), and the radioactivity in the fractions was measured using an automated gamma counter.

Small-Animal PET Studies. Imaging experiments were performed on a Focus 220 microPET scanner (Concorde Microsystems, Knoxville, TN, USA) using male Wistar rats. During all scan sessions, animals were kept under gas anesthesia (2.5% isoflurane in O_2 at 1 L/min flow rate). Dynamic 90-min-scans were acquired in list mode. Acquisition data were Fourier rebinned in 27 time frames (4×15 s, 4×1 min, 5×3 min, 14×5 min) and reconstructed with Filtered Back Projection (FBP). The images were spatially normalized to the rat brain Paxinos coordinate system using affine transformation, allowing the use of a predefined volumes of interest (VOIs) map. Time–activity curves (TAC) were generated for striatum, cortex, cerebellum, hippocampus, thalamus, and total brain for each individual scan, using PMOD software (v 3.2, PMOD Technologies Ltd.). The radioactivity concentration in the different brain regions was expressed as standardized uptake value (SUV) as a function of time π of the radiotracer by normalization for body weight of the animal and injected dose. Rats were injected with about 40–53 MBq of high specific activity formulation of [^{11}C]20f *via* the tail vein under isoflurane anesthesia (2.5% in O_2 at 1 L/min flow rate). For the displacement experiment, a solution of JNJ42153605 in 20% (2-hydroxypropyl)- β -cyclodextrine with 2 equiv of hydrochloric acid was injected iv at a dose of 1 mg/kg 30 min after radiotracer injection.

■ ASSOCIATED CONTENT

● Supporting Information

The different methods used for the LCMS and GCMS characterization of the compounds described in this manuscript; the biodistribution of [^{11}C]20f in normal rats at 2, 30, and 60 min post-tracer-injection; the reconstructed radiochromatogram corresponding to a rat plasma analysis at 30 min postinjection of [^{11}C]20f; and reconstructed radiochromatograms corresponding to a rat perfused cerebrum and cerebellum analysis at 30 min postinjection of [^{11}C]20f. This material is available free of charge via the Internet at <http://pubs.acs.org>.

■ AUTHOR INFORMATION

Corresponding Author

*Tel.: + 34 925 245 780. Fax: + 34 925 245 771. E-mail: iandres@its.jnj.com.

Notes

The authors declare no competing financial interest.

■ ACKNOWLEDGMENTS

We thank José Manuel Alonso, Luis Font, and Alberto Fontana of the Analysis & Purification department in Toledo for their skillful assistance. We also thank Ivan Sannen and Julie Cornelis of the Laboratory for Radiopharmacy, KU Leuven, for their skillful help with the biodistribution and radiometabolite studies, and Ann Van Santvoort, Peter Vermaelen, and Michel Koole of the department of Nuclear Medicine (KU Leuven) for their assistance in the small-animal PET studies. We also thank Heidi Szel, Ilse Biesmans, and Luc Peeters (Janssen R&D, Neuroscience, Beerse) for their expert assistance with the *in vitro* pharmacology studies. Finally, we thank ADDEX Therapeutics for their collaboration on the mGluR2 PAM discovery program.

■ ABBREVIATIONS USED

BBB, blood-brain barrier; CNS, central nervous system; DCM, dichloromethane; ID, injected dose; iv, intravenous; mGlu, metabotropic glutamate; mGluR2, metabotropic glutamate receptor 2; PAM, positive allosteric modulator; PET, positron emission tomography; μ PET, small-animal PET; pi, post injection; RP-HPLC, reversed phase-high performance liquid chromatography; rt, room temperature; SD, standard deviation; SUV, standardized uptake value; TAC, time activity curve

■ REFERENCES

- (1) Conn, P. J.; Pin, J.-P. Pharmacology and functions of metabotropic glutamate receptors. *Annu. Rev. Pharmacol. Toxicol.* **1997**, *37*, 205–237.
- (2) Kew, J. N.; Kemp, J. A. Ionotropic and metabotropic glutamate receptor structure and pharmacology. *Psychopharmacology* **2005**, *179*, 4–29.
- (3) Cartmell, J.; Schoepp, D. D. Regulation of neurotransmitter release by metabotropic glutamate receptors. *J. Neurochem.* **2000**, *75*, 889–907.
- (4) Conn, P. J.; Lindsley, C. W.; Jones, C. K. Activation of metabotropic glutamate receptors as a novel approach for the treatment of schizophrenia. *Trends Pharmacol. Sci.* **2009**, *30*, 25–31.
- (5) Moghaddam, B.; Javitt, D. From Revolution to Evolution: the Glutamate Hypothesis of Schizophrenia and its Implication for Treatment. *Neuropsychopharmacology* **2012**, *37*, 4–15.
- (6) Patil, S. T.; Zhang, L.; Martenyi, F.; Lowe, S. L.; Jackson, K. A.; Andreev, B. V.; Avedisova, A. S.; Bardenstein, L. M.; Gurovich, I. Y.; Morozova, M. A.; Mosolov, S. N.; Neznanov, N. G.; Reznik, A. M.; Smulevich, A. B.; Tochilov, V. A.; Johnson, B. G.; Monn, J. A.; Schoepp, D. D. Activation of mGlu2/3 receptors as a new approach to treat schizophrenia: a randomized Phase 2 clinical trial. *Nat. Med.* **2007**, *13*, 1102–1107.
- (7) O'Neill, M. J.; Fell, M. J.; Svensson, K. A.; Witkin, J. M.; Mitchell, S. N. Recent developments in metabotropic glutamate receptors as novel drug targets. *Drugs Future* **2010**, *35*, 307–324.
- (8) Sheffler, D. J.; Pinkerton, A. B.; Dahl, R.; Markou, A.; Cosford, N. D. P. Recent progress in the synthesis and characterization of group II metabotropic glutamate receptor allosteric modulators. *ACS Chem. Neurosci.* **2011**, *2*, 382–393.
- (9) Wooley, M. L.; Pemberton, D. J.; Bate, S.; Corti, C.; Jones, D. M. The mGlu2 but not the mGlu3 receptor mediates the actions of the mGluR2/3 agonist, LY379268, in mouse models predictive of antipsychotic activity. *Psychopharmacology* **2008**, *196*, 431–440.
- (10) Fell, M. J.; Svensson, K. A.; Johnson, B. G.; Schoepp, D. D. Evidence for the role of metabotropic glutamate (mGlu)2 not mGlu3 receptors in the preclinical antipsychotic pharmacology of the mGlu2/3 receptor agonist (–)-(1R,4S,5S,6S)-4-Amino-2-sulfonylbicyclo[3.1.0]hexane-4,6-dicarboxylic Acid (LY404039). *J. Pharmacol. Exp. Ther.* **2008**, *326*, 209–217.
- (11) Levine, L.; Gaydos, B.; Sheehan, D.; Goddard, A.; Feighner, J.; Potter, W.; Schoepp, D. D. The mGlu2/3 receptor agonist, LY354740, reduces panic anxiety induced by a CO₂ challenge in patients diagnosed with panic disorder. *Neuropharmacology* **2002**, *43*, 294–294.
- (12) Pin, J.-P.; Parmentier, M.-L.; Prezeau, L. Positive allosteric modulators for γ -aminobutyric acid_B receptors open new routes for the development of drugs targeting family 3 G-protein-coupled receptors. *Mol. Pharmacol.* **2001**, *60*, 881–884.
- (13) Gjoni, T.; Urwyler, S. Receptor activation involving positive allosteric modulation, unlike full agonism, does not result in GABA_B receptor desensitization. *Neuropharmacology* **2008**, *55*, 1293–1299.
- (14) Melancon, B. J.; Hopkins, C. R.; Wood, M. R.; Emmitte, K. A.; Niswender, C. M.; Christopoulos, A.; Conn, P. J.; Lindsley, C. W. Allosteric modulation of seven transmembrane spanning receptors: Theory, Practice, and opportunities for Central Nervous System Drug Discovery. *J. Med. Chem.* **2012**, *55*, 1445–1464.
- (15) Trabanco, A. A.; Cid, J. M.; Lavreysen, H.; Macdonald, G. J.; Tresadern, G. Progress in the development of positive allosteric modulators of the metabotropic glutamate receptor 2. *Curr. Med. Chem.* **2011**, *18*, 47–68.
- (16) Passchier, J.; Gee, A.; Willemsen, A.; Vaalburg, W.; van Waarde, A. Measuring drug-related receptor occupancy with positron emission tomography. *Methods* **2002**, *27*, 278–286.
- (17) Wong, D. F.; Tauscher, J.; Gründer, G. The role of imaging in proof of concept for CNS drug discovery and development. *Neuropsychopharmacology* **2009**, *34*, 187–203.
- (18) Wang, J. Q.; Brownell, A.-L. Development of metabotropic glutamate receptor ligands for neuroimaging. *Curr. Med. Imaging Rev.* **2007**, *3*, 186–205.
- (19) Yu, M. Recent developments of the PET imaging agents for metabotropic glutamate receptor subtype 5. *Curr. Top. Med. Chem.* **2007**, *7*, 1800–1805.
- (20) Seneca, N. Recent advances in positron emission tomography imaging of the brain. *Drugs Future* **2011**, *36*, 601–613.
- (21) Fujinaga, M.; Yamasaki, T.; Yui, J.; Hatori, A.; Xie, L.; Kawamura, K.; Asagawa, C.; Kumata, K.; Yoshida, Y.; Ogawa, M.; Nengaki, N.; Fukumura, T.; Zhang, M.-R. Synthesis and evaluation of novel radioligands for positron emission tomography imaging of metabotropic glutamate receptor subtype 1 (mGluR1) in rodent brain. *J. Med. Chem.* **2012**, *55*, 2342–2352.
- (22) Wang, J.-Q.; Zhang, Z.; Kuruppu, D.; Brownell, A.-L. Radiosynthesis of PET radiotracer as a prodrug for imaging group II metabotropic glutamate receptors in vivo. *Bioorg. Med. Chem. Lett.* **2012**, *22*, 1958–1962.
- (23) Cid, J. M.; Duvey, G.; Tresadern, G.; Nhem, V.; Furnari, R.; Cluzeau, P.; Vega, J. A.; De Lucas, A. I.; Matesanz, E.; Alonso, J. M.; Linares, M. L.; Andres, J. I.; Poli, S. M.; Lutjens, R.; Himogai, H.; Rocher, J.-P.; Macdonald, G. J.; Oehlrich, D.; Lavreysen, H.; Ahnaou, A.; Drinkenburg, W.; Mackie, C.; Trabanco, A. A. Discovery of 1,4-disubstituted 3-cyano-2-pyridones: a new class of positive allosteric modulators of the metabotropic glutamate 2 receptor. *J. Med. Chem.* **2012**, *55*, 2388–2405.
- (24) Van der Linden, I.; Peeters, L.; Biesmans, I.; Andrés, J. I.; Vliegen, M.; Te Riele, P.; Langlois, X.; Atack, J. R.; Lavreysen, H. In vitro Characterization of the Binding of the mGlu2 Receptor Positive Allosteric Modulator [³H]JNJ-40068782 to Native and Recombinant mGlu2 Receptors. 7th Int. Meeting on Metabotropic Glutamate Receptors 2011, Taormina, Italy.
- (25) (a) Cid-Nuñez, J. M.; Oehlrich, D.; Trabanco-Suárez, A. A.; Tresadern, G. J.; Vega-Ramiro, J. A.; Macdonald, G. J. 1,2,4-Triazolo[4,3-a]pyridine derivatives and their use for the treatment or prevention of neurological and psychiatric disorders. *PCT Int. Appl. WO2010130424*, November 18, 2010. (b) Cid-Nuñez, J. M.; De Lucas Olivares, A. I.; Trabanco-Suarez, A. A.; Macdonald, G. J. 7-Aryl-1,2,4-triazolo[4,3-a]pyridine derivatives as positive allosteric modulators of mGluR2 receptors and their preparation, pharmaceutical compositions and use in the treatment of CNS disorders. *PCT Int. Appl. WO2010130423*, November 18, 2010. (c) Cid-Nuñez, J. M.; De Lucas Olivares, A. I.; Trabanco-Suarez, A. A.; Macdonald, G. J. 1,2,4-Triazolo[4,3-a]pyridine derivatives as mGluR2 modulators and their preparation and use for the treatment of CNS diseases. *PCT Int. Appl. WO2010130422*, November 18, 2010.
- (26) Manuscripts describing further results of the Medicinal Chemistry exploration around the 1,4-disubstituted-2-pyridones and the 1,2,4-Triazolo[4,3-a]pyridines are in progress and will be reported elsewhere.
- (27) Li, G.; Zhou, H.; Jiang, Y.; Keim, H.; Topiol, S. W.; Poda, S. B.; Ren, Y.; Chandrasena, G.; Doller, D. Design and synthesis of 4-arylpiperidinyl amide and N-arylpiperidin-3-yl-cyclopropane carboxamide derivatives as novel melatonin receptor ligands. *Bioorg. Med. Chem. Lett.* **2011**, *21*, 1236–1242.
- (28) Alcázar, J.; Diels, G.; Schoentjes, B. Reproducibility across microwave instruments: First example of genuine parallel scale up of compounds under microwave irradiation. *QSAR Comb. Sci.* **2004**, *23*, 906–910.

- (29) See ref 25. CA registry no. 1152617-14-5.
- (30) See ref 25. CA registry no. 1254981-17-3.
- (31) See ref 25. CA registry no. 1254981-30-0.
- (32) Pike, V. W. PET Radiotracers: Crossing the Blood-Brain Barrier and Surviving Metabolism. *Trends Pharmacol. Sci.* **2009**, *30*, 431–440.
- (33) Laruelle, M.; Slifstein, M.; Huang, Y. Relationships between radiotracer properties and image quality in molecular imaging of the brain with positron emission tomography. *Mol. Imaging Biol.* **2003**, *5*, 363–375.
- (34) Waterhouse, R. N. Determination of lipophilicity and its use as a predictor of blood-brain barrier penetration of molecular imaging agents. *Mol. Imaging Biol.* **2003**, *5*, 376–389.
- (35) Celen, S.; Koole, M.; De Angelis, M.; Sannen, I.; Chitneni, S. K.; Alcazar, J.; Dedeurwaerdere, S.; Moechars, D.; Schmidt, M.; Verbruggen, A.; Langlois, X.; Van Laere, K.; Andrés, J. I.; Bormans, G. Preclinical Evaluation of ^{18}F -JNJ41510417 as a Radioligand for PET Imaging of Phosphodiesterase-10A in the Brain. *J. Nucl. Med.* **2010**, *51*, 1584–1591.
- (36) Andrés, J. I.; De Angelis, M.; Alcazar, J.; Iturrino, L.; Langlois, X.; Dedeurwaerdere, S.; Lenaerts, I.; Vanhoof, G.; Celen, S.; Bormans, G. Synthesis, *In Vivo* Occupancy and Radiolabeling of Potent Phosphodiesterase Subtype-10 Inhibitors as candidates for Positron Emission Tomography Imaging. *J. Med. Chem.* **2011**, *54*, 5820–5835.
- (37) Method for identification of main metabolites: the test compounds were incubated with human and rat liver microsomes, at 0.4% final solvent concentration (0.16% DMSO and 0.24% MeCN). The study was conducted to identify the main metabolites formed after 0 min (control) and 60 min incubation time in the presence of the NADPH generating system at 37 °C. The test concentration of the compound was 5 μM . Samples were compared to the control incubations, in which compound was added at termination. Data were acquired on a Waters UPLC/QToF Premier mass spectrometer using a 10 min generic UPLC method and a generic MSe method. Complementary MS/MS experiments were performed when necessary. An Acquity UPLC C18 (2.1 mm \times 100 mm, 1.8 μm) column was used. Interpretation of data was performed with Waters Metabolynx software.
- (38) The CEREP selectivity screen was performed on the following targets: SHT_{1A}, SHT_{2A}, SHT₃, SHT_{5A}, SHT₆, SHT₇, A₁, A_{2A}, A₃, AT₁, Beta₁, BK₂, CCKA, CCR₁, D₁, D₂, DAT, ETA, GAL₂, H₁, H₂, IL_{8B}, CXCR₂, M₁, M₂, M₃, MC₄, ML₁, NET, NK₂, NK₃, NPY₁, NPY₂, NT₁, OP₁, OP₃, ORL₁, V_{1A}, VIP, SST, SHT_{1B}, α_1 , α_2 , BZD, CaCH, CICH, GABA, KCH, NaCH, SKCaCH.
- (39) (a) Ohishi, H.; Neki, A.; Mizuno, N. Distribution of a metabotropic glutamate receptor, mGluR2, in the central nervous system of the rat and mouse: an immunohistochemical study with a monoclonal antibody. *Neurosci. Res.* **1998**, *30*, 65–82. (b) Richards, G.; Messer, J.; Malherbe, P.; Pink, R.; Brockhaus, M.; Stadler, H.; Wichmann, J.; Schaffhauser, H.; Mutel, V. Distribution and abundance of metabotropic glutamate receptor subtype 2 in rat brain revealed by [^3H]LY354740 binding in vitro and quantitative radioautography: correlation with the sites of synthesis, expression, and agonist stimulation of [^{35}S]GTPgammaS binding. *J. Comp. Neurol.* **2005**, *487*, 15–27.
- (40) Cid, J. M.; Tresadern, G.; Vega, J. A.; De Lucas, A. I.; Matesanz, E.; Iturrino, L.; Linares, M. L.; Garcia, A.; Andrés, J. I.; Macdonald, G. J.; Oehlich, D.; Lavreysen, H.; Megens, A.; Ahnaou, A.; Drinkenburg, W.; Mackie, C.; Pype, S.; Gallacher, D.; Trabanco, A. A. Discovery of 3-Cyclopropylmethyl-7-(4-phenylpiperidin-1-yl)-8-trifluoromethyl-[1,2,4]triazolo[4,3-a]pyridine (JNJ-42153605): A Positive Allosteric Modulator of the Metabotropic Glutamate 2 Receptor. *J. Med. Chem.* [Online early access]. DOI: <http://dx.doi.org/10.1021/jm3010724>